THE DESIGN AND CONSTRUCTION OF A SIX DEGREE OF FREEDOM PARALLEL LINK PLATFORM TYPE MANIPULATOR

by

AHMAD NAVEED ISMAIL

B.Sc(Hons.) Mech. Engg., N.W.F.P. University of Engineering
and Technology, Peshawar, Pakistan.
(1984)

SUBMITTED TO THE DEPARTMENT OF
MECHANICAL ENGINEERING
IN PARTIAL FULFILLMENT OF THE REQUIREMENTS
FOR THE DEGREE OF

MASTER OF SCIENCE

at the

MASSACHUSETTS INSTITUTE OF TECHNOLOGY

May 1988

Signature of Author _____
Department of Mechanical Engineering
May, 1988

Certified by _____
Igor Paul
Thesis Supervisor

Accepted by _____
Ain A. Sonin
Chairman, Department Committee

THE DESIGN AND CONSTRUCTION OF A SIX DEGREE OF FREEDOM PARALLEL LINK PLATFORM TYPE MANIPULATOR

by

AHMAD NAVEED ISMAIL

Submitted to the Department of Mechanical Engineering
in May 1988 in partial fulfillment of the
requirements for the degree of
Master of Science.

ABSTRACT

A variable admittance, six degree of freedom, parallel linked, hydraulically powered platform was designed, built and tested. The platform spatial mechanism is used to simulate arbitrary base motions of non-stationary robots. The control linkages are six hydraulically operated, computer-controlled, cylinders which operate in a parallel manner to determine the position and attitude of the robot mounted on the top plate. The apparent admittance parameters (stiffness, damping, inertia) of the platform are varied through software such that a wide range of applications can be studied.

For the general control problem, such as position and orientation control of the top plate, the forward kinematic analysis was also investigated. A set of non-linear, mathematical equations were derived and solved iteratively using a multidimensional Newton-Raphson method. Inverse kinematics were used to fine tune the initial guesses to get a standard initial guess value for the Newton-Raphson method. This standard value can be used as a search seed for all the realizable physical positions in the platform's specified workspace.

Thesis Supervisor: Prof. Igor Paul
Title: Associate Professor of Mechanical Engineering

To My Parents
Amee and Abu

ACKNOWLEDGEMENTS

Words are hardly adequate to express my gratitude to Professor Igor Paul, who supervised this thesis. During the course of this work he always listened patiently and critically, regularly offered insightful suggestions and never failed to be enthusiastic and encouraging. I could not have asked for a more supportive and friendly advisor.

I would like to thank Professor Steven Dubowsky for giving me the opportunity and the resources to work on an interesting and practical project.

This thesis benefitted considerably from the work of Moris Fresko and Nathan Stelman, and many discussions with them.

I would also like to thank my friends Egemen Ayna, Joe Deck, Moris Fresko, Dan Lichtenwalner, Andre Sharon, Zia Vafa, Evelyn Vance and Dave Yan for giving me encouragement and making my stay at MIT most enjoyable.

In addition, I thank my fellow students in our research group and the members of Martin Design Center for their friendship, help and valuable technical opinions.

TABLE OF CONTENTS

LIST OF FIGURES

LIST OF TABLES

CHAPTER 1

INTRODUCTION

1.1 OVERVIEW

In the past few years robotic manipulators have gained wide acceptance in industry and have demonstrated their effectiveness in accomplishing many tasks very efficiently. Their usage in tasks which are dangerous or difficult for humans has wide ranging benefits. In such industrial applications current manipulators generally operate in highly structured environments. They are mounted on stationary, rigid bases and are not subjected to base motion disturbances. However, many potential applications, e.g. in space, trucks, tanks, etc., require robots to operate from mobile platforms, and, are therefore subject to arbitrary base motion disturbances.

Many military applications exist which are ideally suited to robotics. The military inherently encompasses tasks which are arduous and dangerous for humans, for which robotic replacements would be advantageous. Similarly, in space, future robotic manipulators are expected to perform tasks such as servicing satellites. Current technology requires that tasks such as repair, construction and maintenance of space stations and satellites be performed by astronaut extra vehicular activity. Using space manipulators would greatly reduce the mission costs and hazards to astronauts [1].

Such applications introduce a number of manipulator control problems not commonly found in today's industrial manipulators. The robotic manipulators mounted on or inside large moving vehicles need to be designed to perform tasks which require precise end effector control. The base motion will subject the vehicle mounted robots to large arbitrary disturbances. These disturbances can degrade the system performance considerably. An important technical difference in the above applications is based on the relative mass differences between the robot and the mobile vehicle. In most military applications, the mass of the vehicle is very much larger than the robot. As a result, the motion of the robot has no substantial effect on the vehicle. Conversely, the motion of manipulators mounted on trucks or spacecraft will cause the base to move. This subsequent robot induced vehicle motion creates additional control problems.

In order to test the developing control theory, a six degree of freedom platform was designed and built. The six degree of freedom platform can simulate the motions of a wide range of moving robot environments. Hence, the dynamic characteristics of a manipulator mounted on this platform will emulate those of various vehicle based manipulators.

1.2 PHYSICAL SYSTEM MODELLING

The physical applications mentioned above can be modelled as a system of inertias (masses), and energy storage and dissipative elements (springs and dampers). The tank motion will not be affected by the robot induced force so we can modelled it as a mass with prescribed motion profile independent of external forces. The truck will exhibit a damped oscillatory

behavior mainly due to its suspension. It can be modelled as a mass supported by a spring and damper with finite coefficients. In the case of spacecraft, the force exerted by the robot base will accelerate the space craft in the direction of the applied force. Therefore, a spacecraft can be modelled as a simple mass (no stiffness or damping). Hence, if the test platform behaves as a programmable mass-spring-damper system with adjustable mass, stiffness and damping coefficients, then any arbitrary physical system can be simulated within the power limits and the response time of the servovalves used to move the platform and the robot.

1.3 CONTENT AND ORGANIZATION

The design specifications for the six degree of freedom platform are given in chapter 2. Chapter 3 essentially discusses the design considerations in selecting a parallel or a serial linkage mechanism. The power requirements and the actuator selection is also given in the same chapter. Chapter 4 discusses the hardware design of the platform, the hydraulic power supply, the servovalve, the instrumentation and the computer hardware used. Chapter 5 presents the kinematic analysis of the six degree of freedom parallel linked mechanism. The solution and the implementation of the forward kinematics is also presented. Chapter 6 discusses the general admittance control for the platform and the modelling of the servo system with experimental verification.

CHAPTER 2

DESIGN SPECIFICATIONS

2.1 IDENTIFICATION OF THE SPECIFICATIONS

System specifications were determined for the range of motion required, the static and dynamic errors, acceleration, bandwidth, accuracy, approximate load carrying capacity, etc.

A robot will be mounted on the top of the platform and the main function of the platform will be to operate under either admittance model or impedance model. The robots to be mounted on the platform are UNIMATION Series PUMA-260 and PUMA-550 [2]. PUMA-250 is shown in Figure 2-1. Some of the basic characteristics of the above mentioned robots to be considered in our design are given in Table 2-1.

The equipment was designed on the worst case scenario by incorporating a mixture of their features so that we won't damage either the robot or the platform. In order not to damage the robot, the acceleration of the platform should not exceed 2 g's and the frequency of the oscillations should not exceed 5 Hz. These two values being the limiting factor for PUMA-250. The platform should be rigid enough so that the robots mounted on the platform can perform their tasks consistent with the accuracy of a comparable robot mounted on a fixed base. In general, as the main function of the platform will be to simulate motion or generate motion so it should be capable of moving in the range 0 to 2 g's.

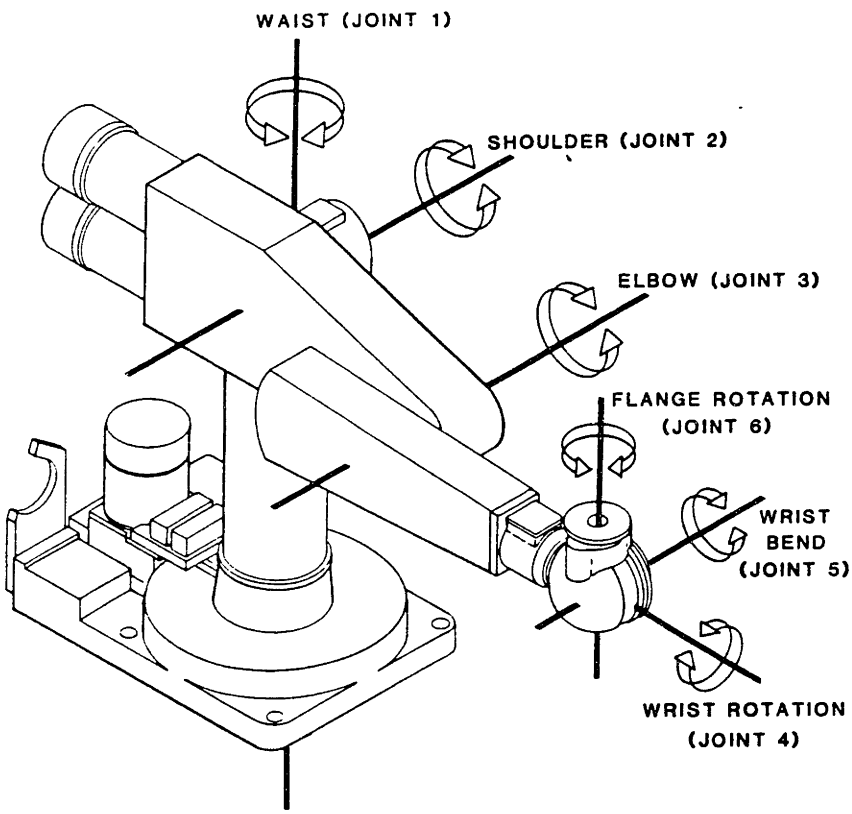

FIGURE 2-1

PUMA-250

CHARACTERISTICS	PUMA-260	PUMA-550
Weight	22 lbs.	132 lbs.
Load Capacity	3.3 lbs.	6.6 lbs.
Position Reoeatability	0.002 in	0.0004 in
Tip velocity with max. load	10 ft/sec	8 ft/sec
Tip acceleration with max. load	75 ft/sec/sec	60 ft/sec/sec
Structural Resonant Frequency	15 HZ	15 HZ

TABLE 2-1

PUMA ROBOT CHARACTERISTICS

Some of the specifications are considered in detail in the following section.

2.2 DETAILED SPECIFICATIONS

2.2.1 WORKSPACE

The workspace is defined as the reachable region of the origin of the moving co-ordinate system embedded in the end effector of the manipulator. The three dimensional workspace is achieved by having six degrees of freedom. The six degrees of freedom is the minimum number required to arbitrarily position an object in space, i.e. three degrees to locate a given point (e.g. (x, y, z) co-ordinates of the center of mass), and three more to

determine the object's orientation within the reference frame (e.g. (φ, θ, ψ) Euler's angles describing rotation). The cartesian and the rotational co-ordinates chosen are shown in Figure 2-2.

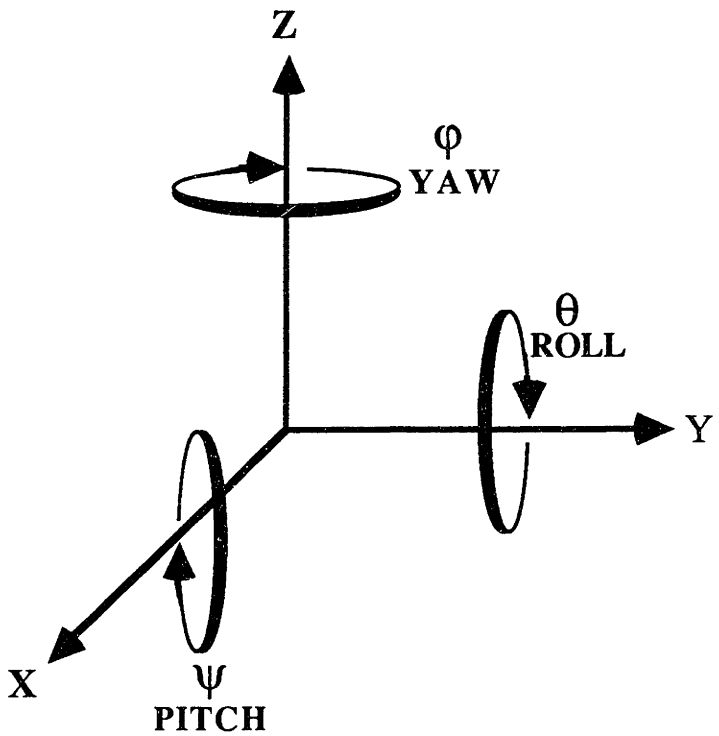

FIGURE 2-2

Reference coordinates

The specifications established for motion in the six degrees of freedom were :

VERTICAL , Z	= ± 6 inches
HORIZONTAL , X	= ± 4 inches
LATERAL , Y	= ± 4 inches
ROLL , θ	= ± 30 degrees

PITCH ,ψ	$= \pm$ 30 degrees
YAW ,φ	$= \pm$ 30 degrees

It should be able to move in any direction singly or in any combination of the six motions. The motion of the platform will be under computer control. Any position profile within the working envelope should be achievable through the computer software. Especially, the combined motions are possible only by the computer as the software will be checking the singular positions and avoiding them.

2.2.2 ACCURACY.

The design specification for accuracy refers to two distinct characteristics: absolute accuracy, and repeatability. Absolute accuracy is the dimensional tolerance which must be allowed the platform in responding to a command given in reference frame coordinates, i.e. the maximum discrepancy between actual position and command position. Repeatability is the maximum discrepancy between responses of the platform to identical position instructions. It measures how faithfully the platform will track a pre-taught trajectory. Note that the absolute accuracy serves as a lower bound for the repeatability specification. Mounting the robot on top of the platform adds another constraint to the design problem. The accuracy of the platform should be atleast equal to or greater than the accuracy of the robot. In our case the lower value of position repeatability for PUMA-550 [see Table 2-1] should be achieved. Therefore, the platform should be rigid enough to be consistent with the robot accuracy.

2.2.3 DYNAMIC RESPONSE

The desired characteristics of the dynamic response of the system are given in the terms of its bandwidth, and the maximum overshoot, rise time, and settling time of the position state variables. The bandwidth of a system gives an indication of its speed of response. It is hoped that the bandwidth of the controlled servo system will be of the order of 5 Hz. The settling time should be fast enough so that it settles down quickly. This means that the transient response is oscillatory and the damping ratio should be in the range of 0.25 -- 0.40. Other transient response characteristics can be defined if one assumed that the system has a dominant pair of poles and so responds like a second order system.

CHAPTER 3

DESIGN CONSIDERATIONS

3.1 DESIGN AIMS

Design aims were to achieve the most simple and cohesive design with the highest capabilities in a wide range of applications. There are many possible designs for providing the six degrees of motion. One obvious method would comprise a three-axis gimbal superimposed upon a three-axis linear slide system. To incorporate rigidity and quick response in this type of solution, when high performance or large amplitudes are required in all of the six motions, generally presents serious design problems and is expensive [3].

There are essentially two main type of robots or manipulators; serially linked and parallel linked. Following is a brief discussion about the two linkages.

3.2 PARALLEL VS SERIAL

Parallel and serially linked manipulators are based upon closed and open chain mechanisms respectively [4]. These two arrangements are illustrated in Figure 3-1 on next page. Traditionally, robots are anthropomorphic, open chain mechanisms. In this mechanism links and joints alternate with one other in a long chain. There are several reasons why the series connected arrangement appeared first. It is a model of the

human arm. This type of manipulator usually has longer reach, larger workspace, and more dextrous maneuverability.

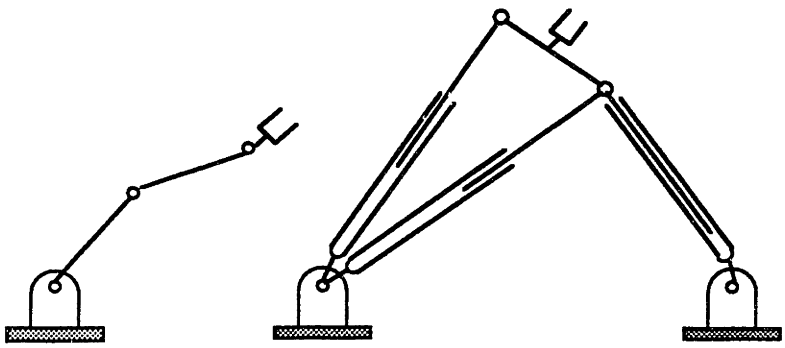

Figure 3-1

Planar Series and Parallel Manipulators

These advantages are paid for with some disadvantages. When the joints are in a fixed position e.g. when you are holding something in your hand, the appendage is cantilever, a very inefficient structure. A pure cantilever is very rarely used as a structure because it must be very massive in order to avoid significant deflection. A cantilever must depend on bending moments to support itself. This leads to limitations on lifting capacity, reduced accuracy and vibration problems. A second disadvantage is that the positions of the links are usually indeterminate. This means that with gripping mechanism in one position the other links can be in many positions. This causes a control problem with multiple solutions to the equations of motion. Another control problem results when the device is moving at a high speed and must come to stop in a precise location without overshoot.

Parallel linked or closed kinematic chain is an alternative in which the links and the joints are composed into two or more chains connecting the base of the manipulator with the end effector. There are also combinations in which part of the manipulator is serial and part parallel. Some advantages and disadvantages of parallel configuration are listed below [5], [6], [7].

3.2.1 ADVANTAGES

1. Very high strength/stiffness-to-weight ratios can be achieved because actuating links bear no moment loads, but are simple tension-compression members.

2. Since the actuators act in parallel, rather than series, to position the end effector, the force and moment capacity of the manipulator is much higher than that of the individual servomotors. A serial link arm is no stronger than its weakest link or joint actuator.

3. Manipulator inertia is minimal. Bulky links and massive motors are not being waved about in space - only the end effector. This results in economy of power and superior dynamic performance.

4. High accuracy results from the geometry: actuator errors are not multiplied by long linkage arms to determine endpoint tolerances: rather, the end effector offset is normally of the order of actuator offset, due to their direct connection.[1]

---

[1] Generally true, but not without exceptions. Near singular points (vanishing of the inverse kinematics' Jacobian determinant) small perturbations in actuator length may give rise to relatively large offsets of the end effector.

5. Simplicity results from the direct connection between the actuators and end effector. No complex drive trains are necessary. This pays dividends in cost reliability, and performance - friction and backlash is minimal.

6. The inverse kinematics are easy, allowing control of the manipulator with a small microprocessor.

3.2.2 DISADVANTAGES

1. The principal disadvantage of the parallel linkage is the difficulty in reaching into small holes or around corners. This type of work is not common, and the deficiency can be partially compensated by an extension attached to the end effector.

2. The length of reach and range of motion are relatively smaller than the open chain mechanism for the same amount of hardware.

3. At extended reach, near the aforementioned singular points, loading of the manipulator can give rise to high tensile and compressive loads in the actuators.

There is one another major difference between the series and parallel arrangements. This is in the mathematical models. For the series connected mechanism the equations as written give the end effector position in terms of the joint variables. For the parallel connected mechanism the equations as written give the joint variables in terms of the end effector position. In a robot the basic control task is to position the end effector; this requires equations for the joint variables in terms of the end effector position. Therefore, the equations for the series manipulator must be inverted (solved)

while those for the parallel manipulator are used as is. Thus the equations for the parallel machine are more easily obtained.

The closed kinematic chain manipulator have potential applications where the demand on workspace and maneuverability is low but the dynamic loading is severe and high speed and precision motion are of primary concerns.

Our requirements need a strong and flexible base to shake and move around a robot weighing roughly 132 lbs. at 2 g's. Using a serially linked mechanism will require a massive structure to have enough force and moment capacity to satisfy our needs. Therefore, after studying the pros and cons of both mechanisms with respect to our design specifications, we decided to use closed kinematic chain mechanism. The closed kinematic chain selected for our spatial motion needs is called Stewart mechanism. Figure 3-2 on next page shows a Stewart Platform in its simplest form. It is a spatial mechanism consisted of a fixed plate and a moving plate connected together by six adjustable links. The joints at both ends of each link allow general rotation. Stewart originally suggested this mechanism as an aircraft simulator platform.

3.3 STEWART MECHANISM

The Stewart platform is a space truss. A truss has larger load bearing capacity (for a given deflection) and fewer vibration problems because it depends on tension and compression in its members instead of bending as a cantilever does. Stewart mechanism is essentially an octahedron with two opposite faces as the rigid base and movable platform [3]. The other faces are

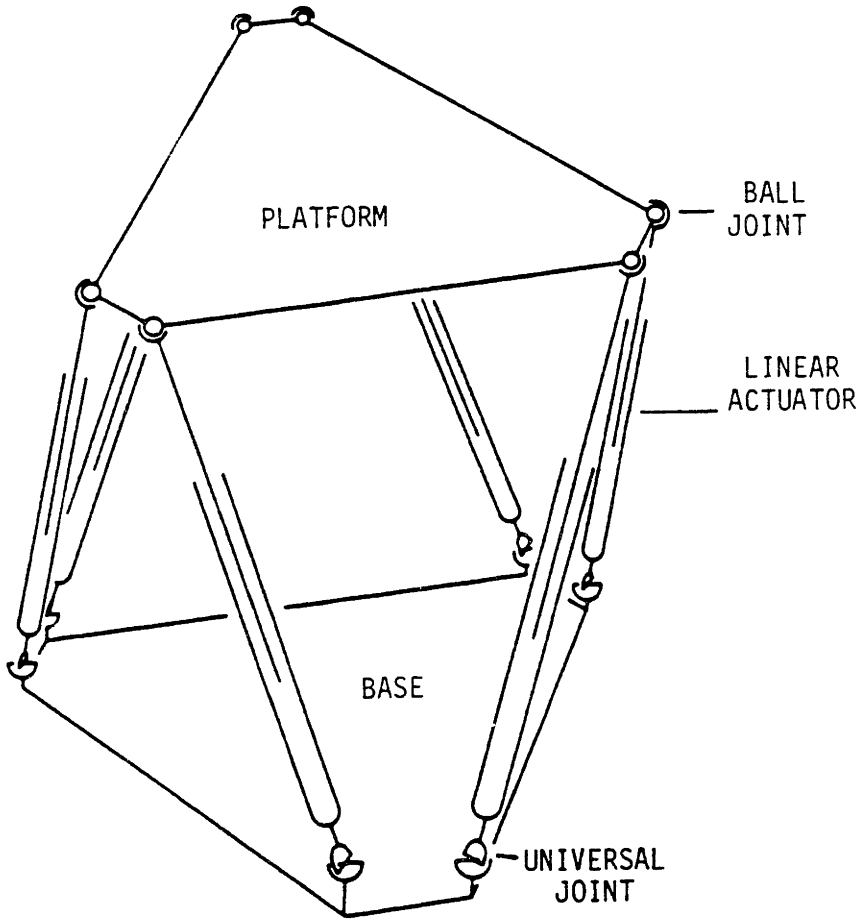

Figure 3-2

Simple Stewart Mechanism

open; the six edges that outline these faces are linear actuators. With the base fixed the platform can take any position and any orientation within a limited volume of space.

An arrangement of Stewart kinematic linkage which has the required six degrees-of-freedom is shown in Figure 3-3. The fixed and moving bodies are hexagonal figures with Hooke's joints (Universal joints) and Spherical joints (ball joints) having two and three degrees of freedom respectively. The connection between the two bodies is completed by six pairs of links, each pair connected by a prism joint (linear actuator). The resulting mechanism has 14 links, 18 joints, and a total of 36 degrees of freedom in them.

TYPE OF JOINT	NO. OF JOINTS	DEGREES OF FREEDOM PER JOINT	DEGREES OF FREEDOM
SPHERICAL	6	3	18
HOOKE'S	6	2	12
PRISMATIC	6	1	6
		TOTAL =	36

TABLE 3-1

DEGREES OF FREEDOM IN JOINTS OF A GENERAL SIX DEGREE OF FREEDOM LINKAGE

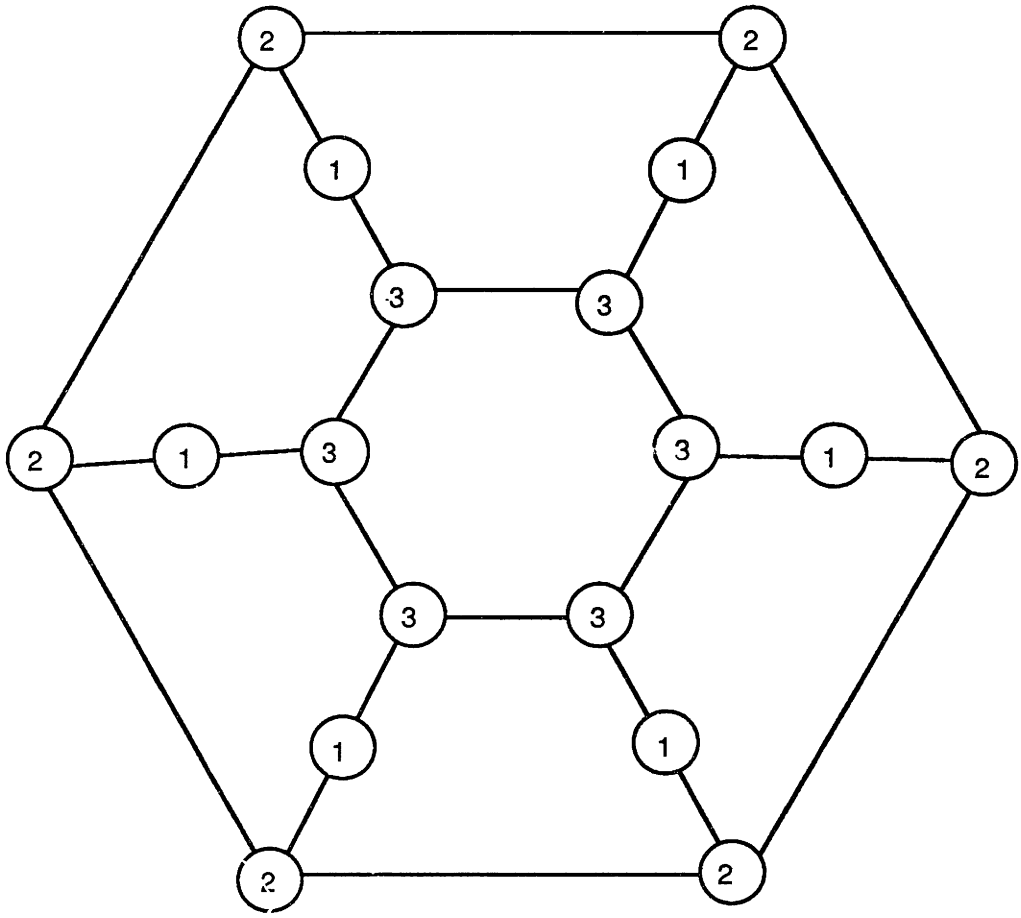

FIGURE 3-3

General Six Degree of Freedom, Fourteen Link Stewart Mechanism. Numbers show degrees of freedom in the joints

In order for the Stewart platform to operate as a six degree-of-freedom mechanism each of the six legs (connections) must have connectivity (mobility of one end of the connection with respect to the other) six. This can be demonstrated with the standard spatial mobility Kutzbach criterion [5], [8]. This criterion asserts that

$$F = 6(n-1) - \sum_{j=1}^{g} (6 - f_j)$$

where

F = degrees of freedom in the system

f = number of degrees of a joint

n = number of links

g = number of joints

For the case where all the prismatic joints are free, it can be demonstrated that the total linkage has a mobility of six:

$$n = 14$$

$$n = 18$$

and

$$F = 6(14-1) - \left[\sum_{j=1}^{6} (6-3) + \sum_{j=1}^{6} (6-2) + \sum_{j=1}^{6} (6-1) \right]$$

or

$$F = 6.$$

Whereas, for the case in which all of the prismatic joints are locked

$$n = 8$$

$$g = 12$$

and

$$F = 6(8-1) - \left[\sum_{j=1}^{6} (6-3) + \sum_{j=1}^{6} (6-2) \right]$$

or

$$F = 0.$$

Furthermore, it can be shown that the degrees of freedom can be reduced by one everytime one of the prismatic joints is locked, until in general, a structure is obtained, when all of the variable links are fixed. This means that the position of the movable body is uniquely given by a set of six lengths.

3.4 POWER REQUIREMENTS

To estimate the power required to operate the platform, we assume the system is following a sinusoidal position profile. The displacement of the platform is then given as

$$x(t) = A \sin(2\pi f t) \qquad (3.1)$$

where f is frequency (Hertz)

A is Amplitude (inches)

π is 3.1415926

The velocity and acceleration of the platform are given respectively by

$$v(t) = 2\pi f A \cos(2\pi f t) \qquad (3.2)$$

and

$$a(t) = -4\pi^2 f^2 A \sin(2\pi f t) \qquad (3.3)$$

As one of the limiting constraint in order to prevent damage to the robot is that the acceleration of the platform should not exceed 2 g's, therefore the maximum acceleration is given by the expression

$$a(t)_{max} = -4\pi^2 f^2 A = 2g \qquad (3.4)$$

where g is acceleration due to gravity = 386 in/sec^2

The frequency f is then solved in terms of the amplitude A and plotted in Figure 3-4. The curve defined by equation (3.4) defines the allowable range of operation.

The power required to move a mass M is given by

$$P(t) = (\text{Force})(\text{Velocity})$$

$$= M\,a(t)\,v(t)$$

Maximum power is then given by

$$P(t)_{max} = (4\pi^2 M) f^2 A^2 \qquad (3.6)$$

By substituting f from equation (3.4) into (3.6.), it can be seen that, if the magnitude of the acceleration is limited to 2 g's then the maximum power consumption is proportional to the square root of the maximum amplitude, which in case is specified as 6 inches. Assuming that the total weight of the robot, top plate, top joints and the force sensor is approximately equal to 300 lbs, hence M = 300 lbs. Therefore from equations (3.5) and (3.6), the maximum power required to drive the platform is approximately 20 horse powers.

3.5 ACTUATOR SELECTION

There are three main types of actuating systems, namely; electro-mechanical, pneumatic and hydraulic [9].

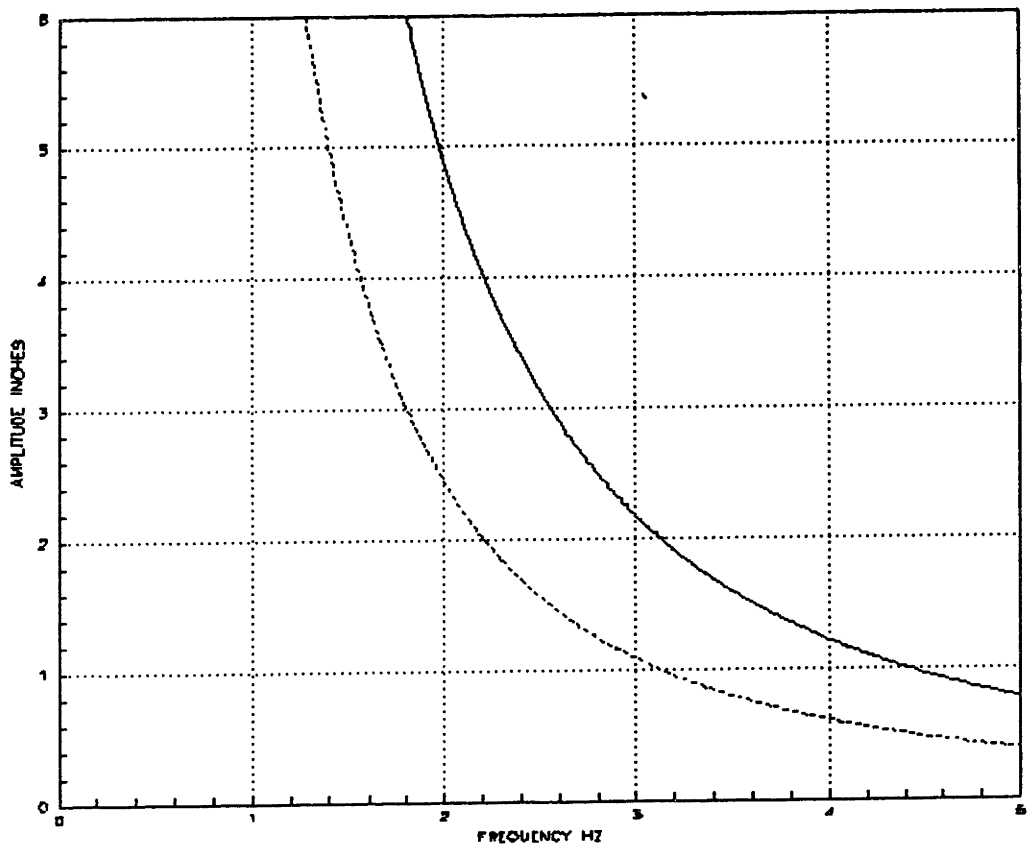

FIG 3-4

Frequency vs. Amplitude Curve

Of the three actuating systems, pneumatic is clearly the worst choice for our application. The major drawback is the compressibility of the working fluid. Any friction in the actuators would cause a build up of pressures prior to any displacement, which, in turn, would tend to result in a slip-stick type of motion. The maximum velocity of the actuators can be controlled, the acceleration to maximum velocity cannot. Neither can the position in the cylinder, at which the maximum velocity is attained, be accurately predicted. As a result the motion is considerably non-linear. Achieving a bandwidth of 1 Hz. might also prove to be impossible due to the cushioning action. There is an another problem, noise -- and it occurs at the venting orifices due to the exhaust of high pressure air to atmospheric pressure.

A electro-mechanical system would also appear to have several significant drawbacks. Although, stepper motors and continuous-motion motors are very suitable for computer control. They are safe, clean, small, reliable, and quiet. The rotary output of the motor has to be converted into linear through some sort of mechanism and this becomes very difficult for the velocities and the accelerations specified. Friction and backlash could be reduced to acceptable levels by using ball screws as opposed to worm or helical gears. The required positioning accuracy could no doubt be achieved with ball screws, since they are used in machine tools that have positioning accuracies of 0.0001 - 0.002 inches. The maximum recommended angular speed for screw is about 3000 RPM. Operating above this level will cause excessive heat and wear. To obtain linear velocities in the order of 60 inches/sec, the ball bearing leadscrew must have a lead greater than 1 inch.

Screws this large are very expensive and have high inertia. Packaging a mechanism of six motors and six independent variable links would also be a problem.

Of the three types of actuating systems, a hydraulic system would seem to be preferable. It has the obvious advantage over a pneumatic system of a virtually incompressible working fluid. Also, much greater force can be transmitted by similar-sized components compared with those used for pneumatic systems. In general, hydraulic systems are reliable, rugged, powerful, fast in response and has highest power/weight ratio of any prime mover. They tends to be messy due to oil leakages. Another disadvantage is that the rigidity of the variable links using hydraulic actuators would be less than using electro-mechanical actuators. The feasibility of using hydraulics in a computer controlled environment is supported by the existence of hydraulic numerical control machines which have accuracies in the range of 0.0001 to 0.002 inches. We decided to implement hydraulics as the actuating system due to its obvious advantages over other systems and also because a hydraulic power supply was conveniently available to us.

CHAPTER 4

HARDWARE DESIGN

This chapter describes the construction of the platform: the design problems and their solutions. The platform has been constructed not as a prototype, but as a functional piece of hardware to emulate the robot base motion. Figure 4-1 and 4-2 shows the photographs of the completed six degrees of freedom parallel linked platform.

4.1 PLATFORM DESIGN

The platform structure essentially consists of hexagonal base connected to the top plate via six hydraulic servo-actuators with joints on each end. The actuators are grouped into three pairs, each consisting of two adjacent actuators connected together at the top. Hence the six degrees of motion can be determined, for if the three connection points in the top plate are moved similarly in the X-Y-Z coordinates, the three linear motions are obtained and if moved in the X-Y-Z coordinates differentially then the three angular motions are obtained. The end of the legs in base are arranged in a plane, as are the end of the legs in the platform. Each leg of the platform has six degrees of freedom individually; as the base is fixed so two degrees lie in the joint connecting the base to the actuator, one in the actuator and the last three in the joint connecting the actuator to the top plate.

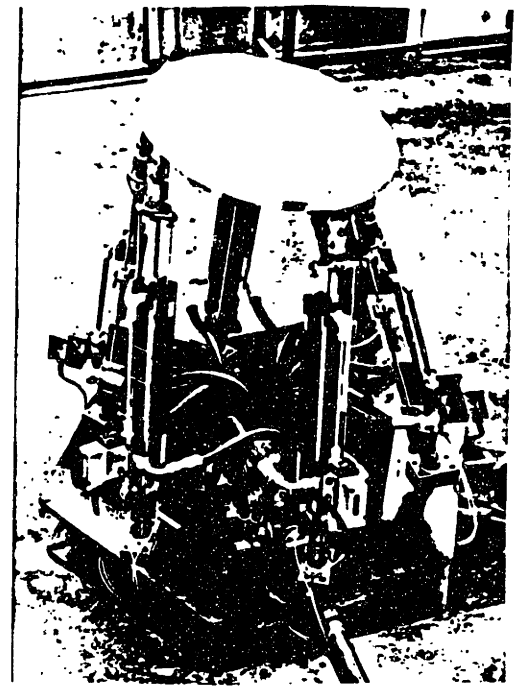

Figure 4-1

Completed 6 DOF Platform

Figure 4-2

6 DOF Platform

It is apparent that the linear displacements of the platform are directly related to the amplitude of movement of the actuators, whereas the amplitudes of the angular attitudes will be proportional to the spacing of the actuator joints on the top plate relative to the linear motions of the actuators. Therefore, the smaller the size of the top plate relative to the stroke of the actuators, the larger the angular motions. A restriction on the choice of the joints position is that if the points in base and the top plate are at the corners of regular planar hexagons, the platform is not always constrained relative to the base and is structurally unstable. Thickness of the joints also pose a physical constraint in designing the top plate because close location of the joints would be difficult to design and implement and also it might hinder the motion of the joints.

The accuracy with which we can specify the location of the top plate of the platform clearly depends on the rigidity of the work station's structural members, the clearances on its joints, and the dimensional tolerances of its components [10]. Considerable care was taken in this regard to achieve the maximum accuracy possible.

Basic components of the platform are discussed briefly in the following sections.

4.1.1 BASE PLATE

The positioning of the base points relative to the top support points will influence the shape of the total envelope of movement. The plane containing the legs when in the mean position contains the base and top

support points, and a choice of positioning the base point within the plane can be made.

If the base joints are positioned directly below the top plate support points, the envelope of movement is confined above the plane containing the base points and the amplitude is larger in the horizontal plane than in the vertical direction. Alternatively, if the base joints are positioned in the same plane as that containing the top support points, the envelope of the movement lies above and below this plane and the amplitude will be larger in the vertical direction than the horizontal plane. After considering all the positions we decided to use a regular hexagon for the base and a semi-regular hexagon for the top plate. The plane in which these hexagons lie are the z = 0 planes in the base and the top coordinates systems. This positioning of the joints gives us maximum workspace envelope for our given design specification.

The center of the six base joints are located 60 degrees apart on a circle of radius 18 inches, Figure 4-3.

The base is constructed from 8 inches, wide flange, I-beam made of carbon steel. Six symmetrical pieces of I-beam were welded together to form a regular hexagon, see Figure 4-4. Location of the holes drilled for the attachment of mounting blocks are also shown in the Figure 4-4.

4.1.2 JOINTS

Joints play an important part in determining the flexibility of the movements of the platform. The joints are connected at the bottom and top of

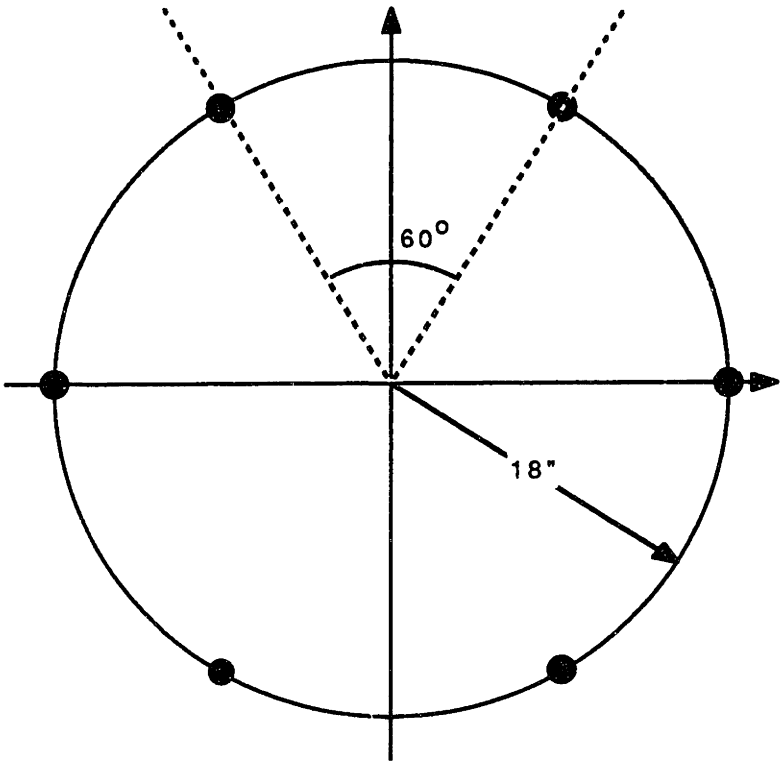

FIGURE 4-3

Location of center of base U-joints

each actuator. The base and top joints have two and three degrees of freedom respectively. The base joints used were 2" outer diameter, Universal joints having $\pm 37^{o}$ operating angle. The U-joints were welded in 1" thick base blocks at an angle of 16^{o} relative to z-direction, see Figure 4-5. The base blocks are mounted on the base in pairs at an angle of 28^{o} facing each other, see Figure 4-4.

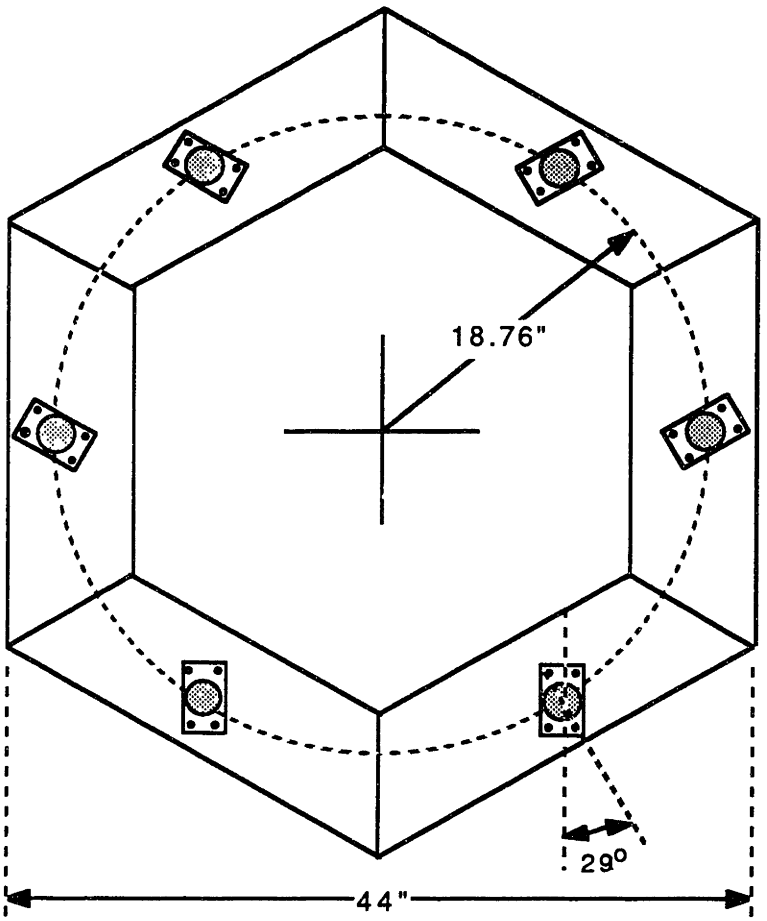

FIGURE 4-4

Platform Base

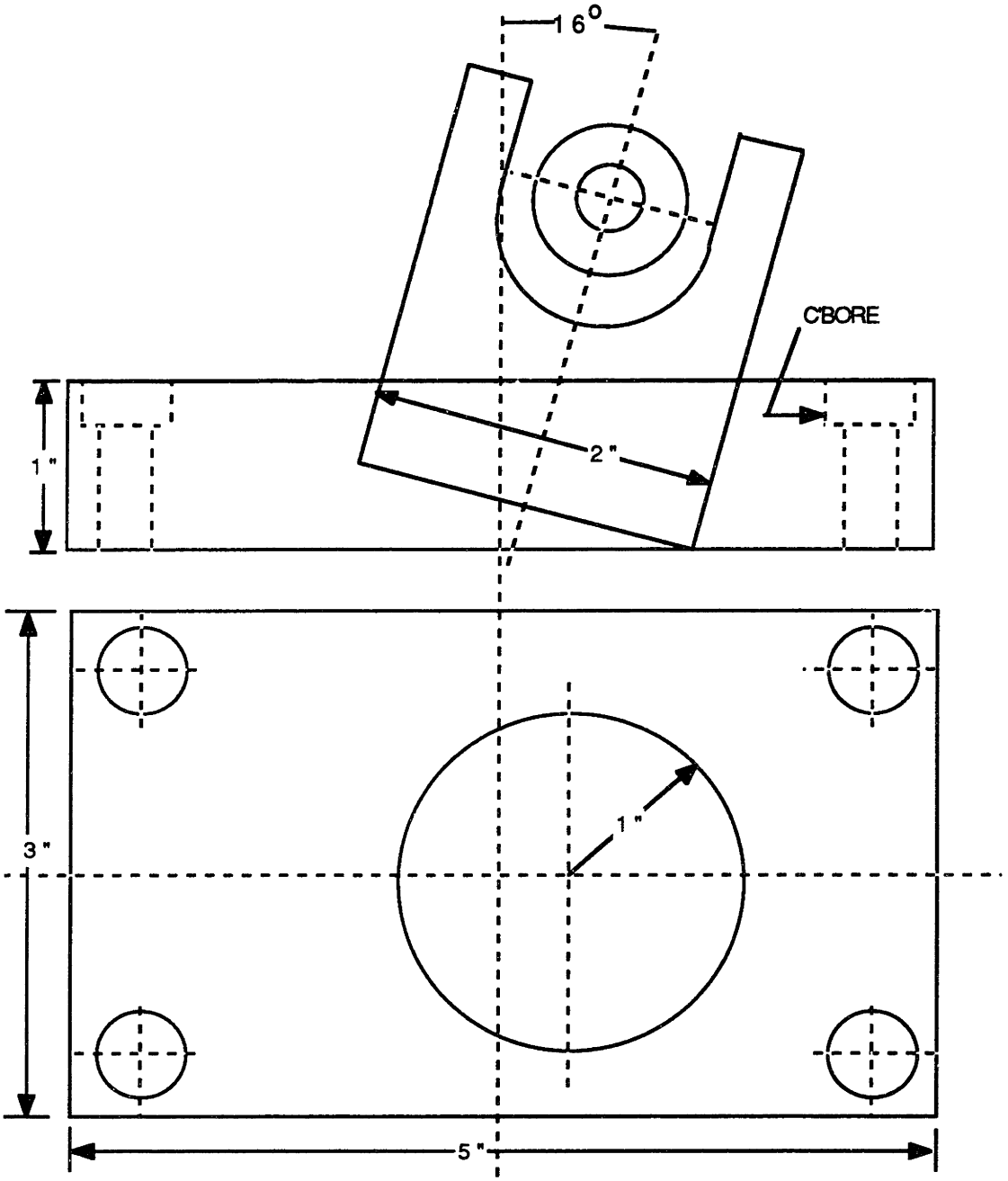

FIGURE 4-5

Base Joint and Base Plate

The length of the actuator at zero stroke from the center of base joint to center of top joint is equal to 31". The top joint is at an angle of 11° from the horizontal top plate. Figure 4-6 shows Elevation in plane containing both joints of one link.

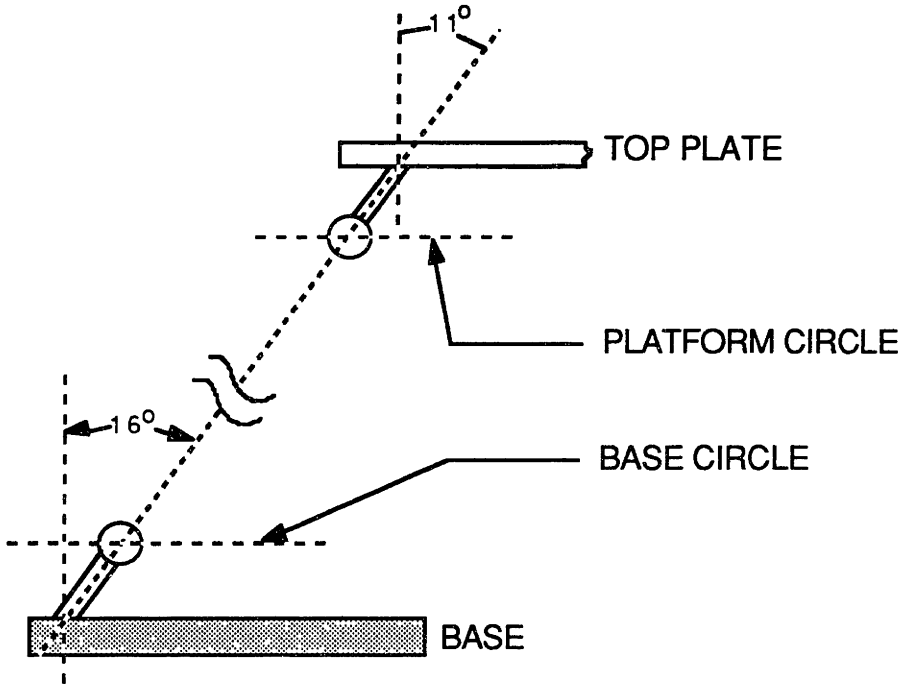

FIGURE 4-6

Base and Top Joint Orientation

Since we need three degrees of freedom in the top joint, ideally a ball joint would have been perfect as it can move freely with respect to all three Cartesian axes. In practice, however, this is not true. The motion of the ball joint is always restricted because of its physical dimensions. The physical constraints imposed by the socket to hold the ball, restrict the rotatability of

the joint in the vertical plane. In order to overcome this problem a new joint was designed, see Figure 4-7.

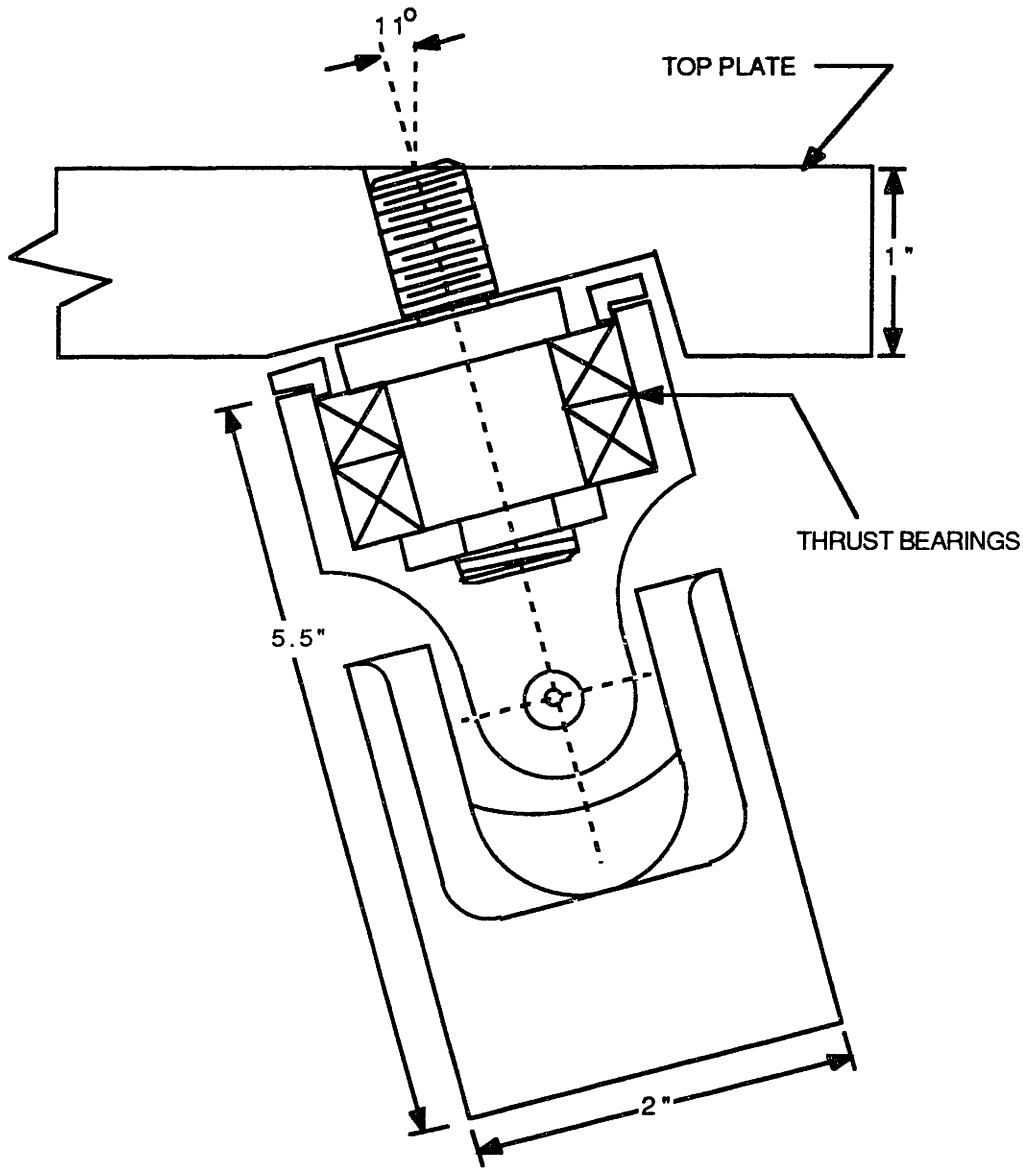

FIGURE 4-7

Top Joint Design

This top joint consists of a specially machined 2" outer diameter Universal joint. These U-joints have an operating angle of $\pm 45^{o}$ and in the two perpendicular planes of rotation can bend outdo $\pm 90^{o}$. The plate side of the U-joints were machined internally to hold two 1.57" O.D. Tapered Roller bearings (TIMKEN-TS TYPE LM11749). These bearings essentially carry a combination of radial and thrust loads, see Figure 4-7. The joints are connected in three pairs and the angle of separation between two joints in a pair is 36^{o}. The center of the top joints are located in a circle of radius 11" and joint pairs are separated by an angle of 120^{o}. As stated earlier, the top joints make a semi-regular hexagon, see Figure 4-8.

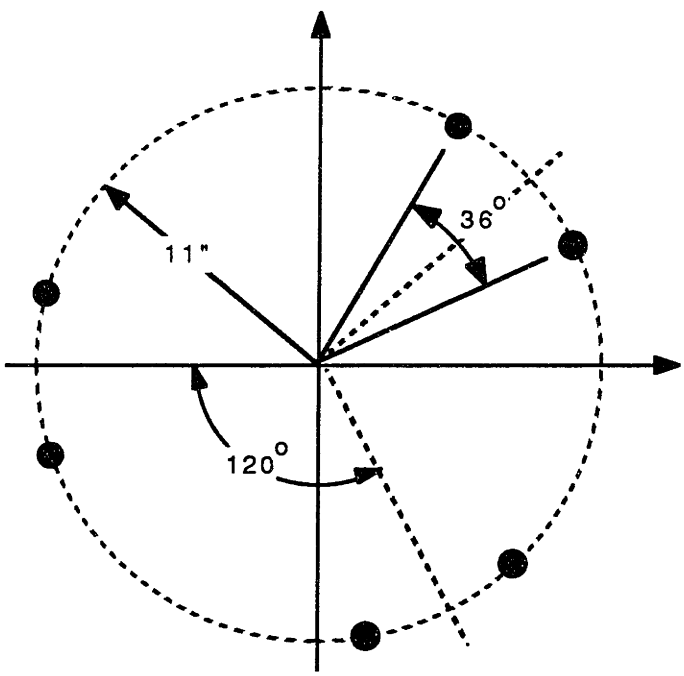

FIGURE 4-8

Top Joints Location

4.1.3 TOP PLATE

The top plate is made of 1 inch Aluminum. Holes were drilled and tapped for the attachment of the top joints. The design and the location of the holes is shown in Figure 4-9. In addition to the joints, the plate will also be carrying the force sensor and the robots will be mounted on top of the force sensor. In order to get the desired accuracy, the machining of the plate was done on a Numerically controlled milling machine.

4.2 HYDRAULIC POWER SUPPLY

In order to calculate the hydraulic power supply requirements, platform was assumed to follow a sinusoidal position profile, as already discussed in chapter 3. Frequency, velocity and fluid flow per cylinder were then calculated using simple fluid flow equations, see Table 4-1.

From the table, we see that in order to meet the design specifications of having atleast ± 6" of amplitude in the z-direction and an acceleration of 2g's, we need 7.7 gpm of hydraulic fluid per cylinder. Therefore, for six cylinders at ± 6" stroke, we need

33.6 gpm ----> 1 g acceleration

and 46.2 gpm ----> 2 g acceleration.

Since the platform will be moving in all the six degrees of freedom, it will be utilizing the maximum stroke of the cylinders i.e. ± 9". The fluid flow rate at this stroke value for an acceleration of 2 g is 57.6 gpm. Hence, a hydraulic power supply unit capable of supplying 60 gpm at 2000 psi will adequately satisfy our design requirements.

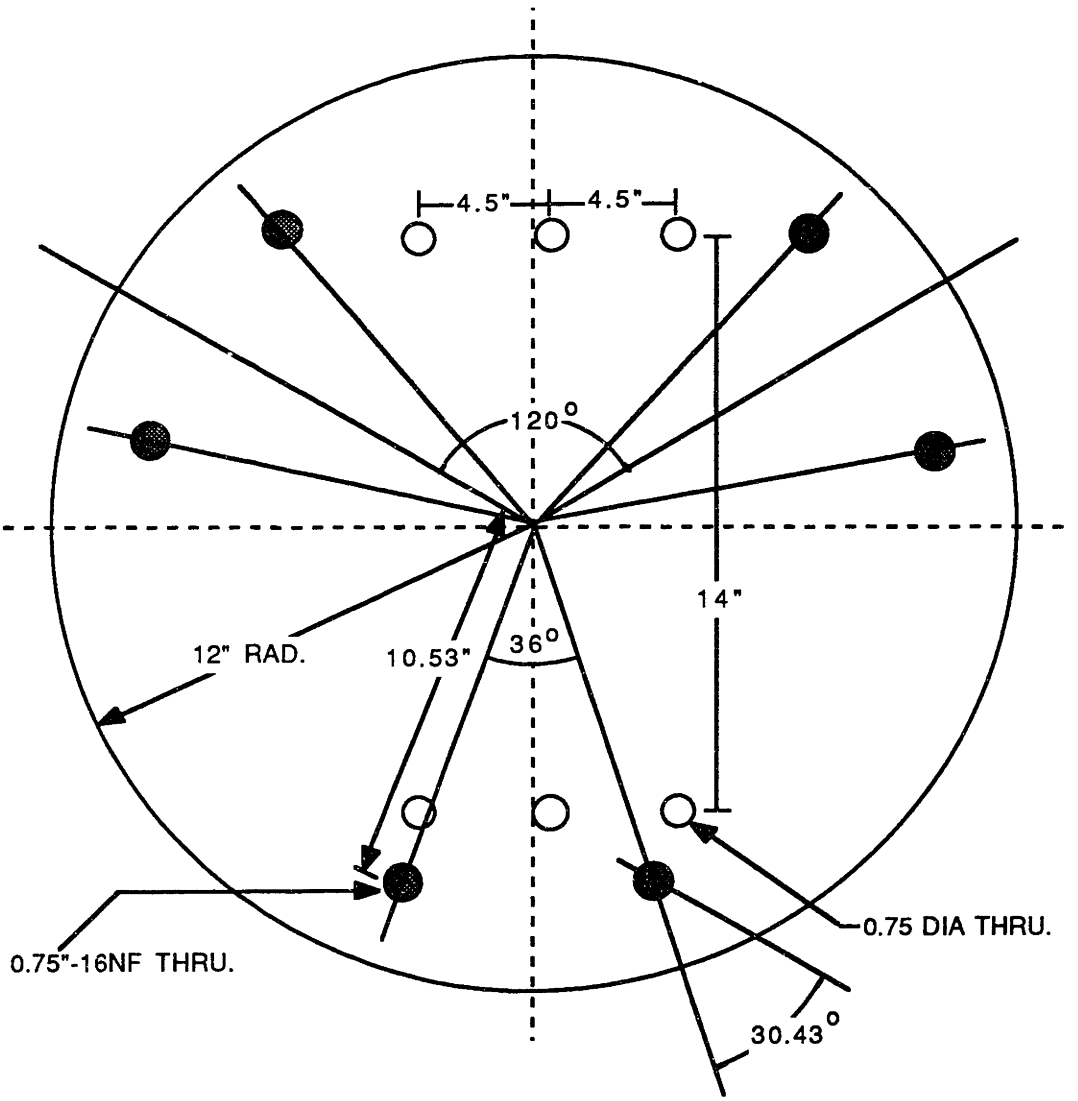

FIGURE 4-9

Top Plate Design

STROKE		± 3"	± 6"	± 9"
1 g	f (Hz)	1.8	1.3	1.04
	V (in/s)	33.9	49	59
	Q (gpm/cyl)	3.86	5.6	6.7
2 g	f (Hz)	2.6	1.8	1.5
	V (in/s)	49	67.8	84.8
	Q (gpm/cyl)	5.6	7.7	9.6

TABLE 4-1

Hydraulic Calculations

As a smaller hydraulic power supply unit was conveniently available to us, the platform was hooked up to this unit until the purchase of the desired 60 gpm unit. The unit can deliver a flow rate of 22 gallons per minute at 500 psi pressure. The power supply delivers constant pressure which can be varied by adjusting the relief valve. The hydraulic power supply unit is assembled and delivered by Kennet Corporation and is schematically shown in Figure 4-10. Appendix A1 gives detailed specifications about the hydraulic power supply.

In order to keep system losses at a reasonably low value, the hydraulic lines were kept as short as possible and the oil velocity should be less than 20 ft/sec at all times.

4.3 SERVOVALVE AND HYDRAULIC CYLINDER

The problem of properly matching a servovalve and actuator to its load is very important. If the servovalve is too small, the system may become velocity limited during its duty cycle and may have poor dynamic response. This is mainly due to a large pressure drop that occurs across the servovalve instead of across the actuator connected to the load.

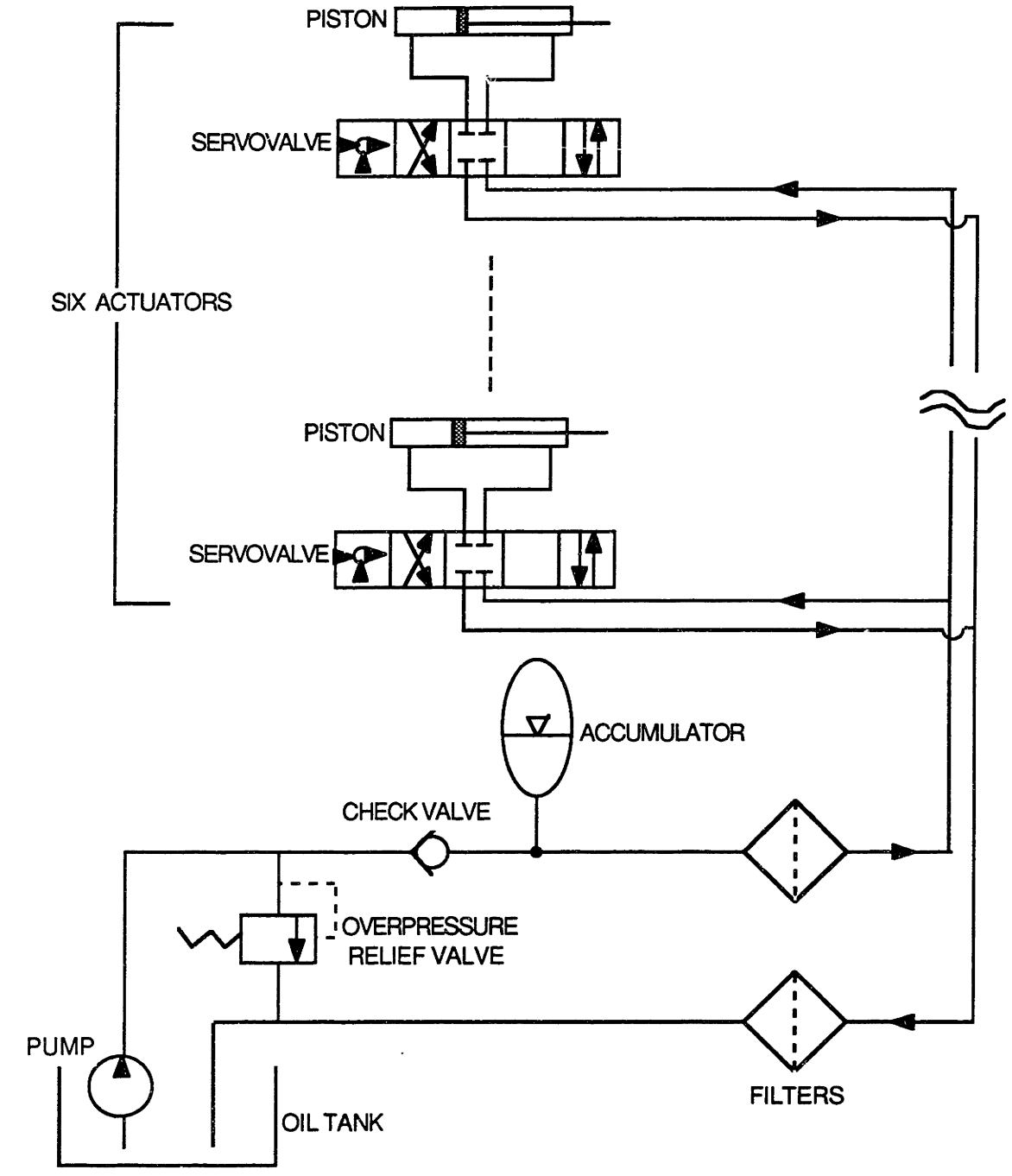

FIGURE 4-10

Schematic of Hydraulic Power Supply

In general, the maximum power that a valve can deliver to the load occurs when the load differential pressure equals two-thirds of the supply pressure (i.e. for max. power transfer, operation best = 2/3 supply pressure). Neglecting losses, the remaining one-third of the system pressure drop occurs across the servovalve. Therefore, in order to get atleast 2000 psi working supply pressure for each actuator, servovalves with a supply pressure of 3000 psi were selected for the platform.

The servovalves used are MOOG High Performance 620-820 series flow control valves. One servovalve is connected to each actuator and the power supply. The frequency response at 3000 psi for $\pm$100% signal is greater than 20 Hz (-3 dB Amplitude). See sevovalve specifications in Appendix A2. The modelling aspects are discussed in the Chapter 6.

The actuators used are Parker Type H2HTS24-18 Heavy duty hydraulic cylinders with low friction seals. The cylinder bore is 1.5 inches, stroke 18 inches and the rod diameter is 1 inch. The maximum operating pressure is 3000 psi in pull application. The servovalves were mounted on top of the cylinders to reduce the pressure loss in the pipes.

4.4 INSTRUMENTATION

There are two different kinds of feedback coming back to the computer for the monitoring purposes i.e. position feedback and force feedback. The measurements are the linear displacement of each actuator and the force exerted by the robot base on the platform. A Linear Motion Position Transducer is connected to each actuator to measure the varying stroke. The potentiometer specifications is given in Appendix A3.

An AMTI Multi Component Transducer of type MC12 Series is used for the force and moment measurement. The transducer measures the six components of force and moment: the downward force, the horizontal forces, and their associated moments. Electrical output signals proportional to those components are obtained through the use of 100 lb rated metal foil strain gage load cells built inside the sensor. The force transducer attached to the center of the top plate and the robots will be mounted on top of it. Some specifications for the force sensor are given below:

Capacity:	F_x, F_y	= 200 lbs
	F_z	= 400 lbs
	M_x, M_y	= 2400 in-lb
	M_z	= 1200 in-lb
Sensitivity:	F_x, F_y	= 6 microvolts/volt-lb
	F_z	= 1.5 microvolts/volt-lb
	M_x, M_y	= 0.6 microvolts/volt-in-lb
	M_z	= 1.3 microvolts/volt-in-lb
Stiffness $x(10^{-6})$:	60,000 lb/in	
Resonant Frequency:	F_x, F_y	= 300 Hz
	F_z	= 600 Hz

4.5 COMPUTER EQUIPMENT

A Digital Equipment Corporation PDP 11/73 micro-computer [11] is used to control the platform, acquire data, and communicate with the controller of the robot which is mounted on the platform. Figure 4-11 shows the internal hardware of the computer. The computer uses a 16 bit processor with a RAM

memory of 512 KB. It runs on the RT-11 operating system and real time programming is done in Pascal language [11].

A Digital Equipment Corporation KWV11-C Real Time Clock board is used to time and synchronize control loops, so that they run at constant rates. The module will count at frequencies ranging from 100 Hertz to 1 MHz.

Two Digital Equipment Corporation AXV11-C Analog Input/Output boards and one AAV11-C board is used to perform the A/D and D/A conversions. In AXV11-C board, the A/D converter accepts up to 16 single-ended inputs, or up to 8 differential inputs, and its D/A converter has two channels. The input and output voltages are within plus or minus 10.0 volts in the 'Offset Binary' configuration. The AAV11-C board is a D/A converter and has 4 channels. It has also a DRV11-J 64 line parallel and a DLVJ1 4 channels serial I/O boards.

Appendix A4 gives the timings for some of the operations possible on PDP 11/73.

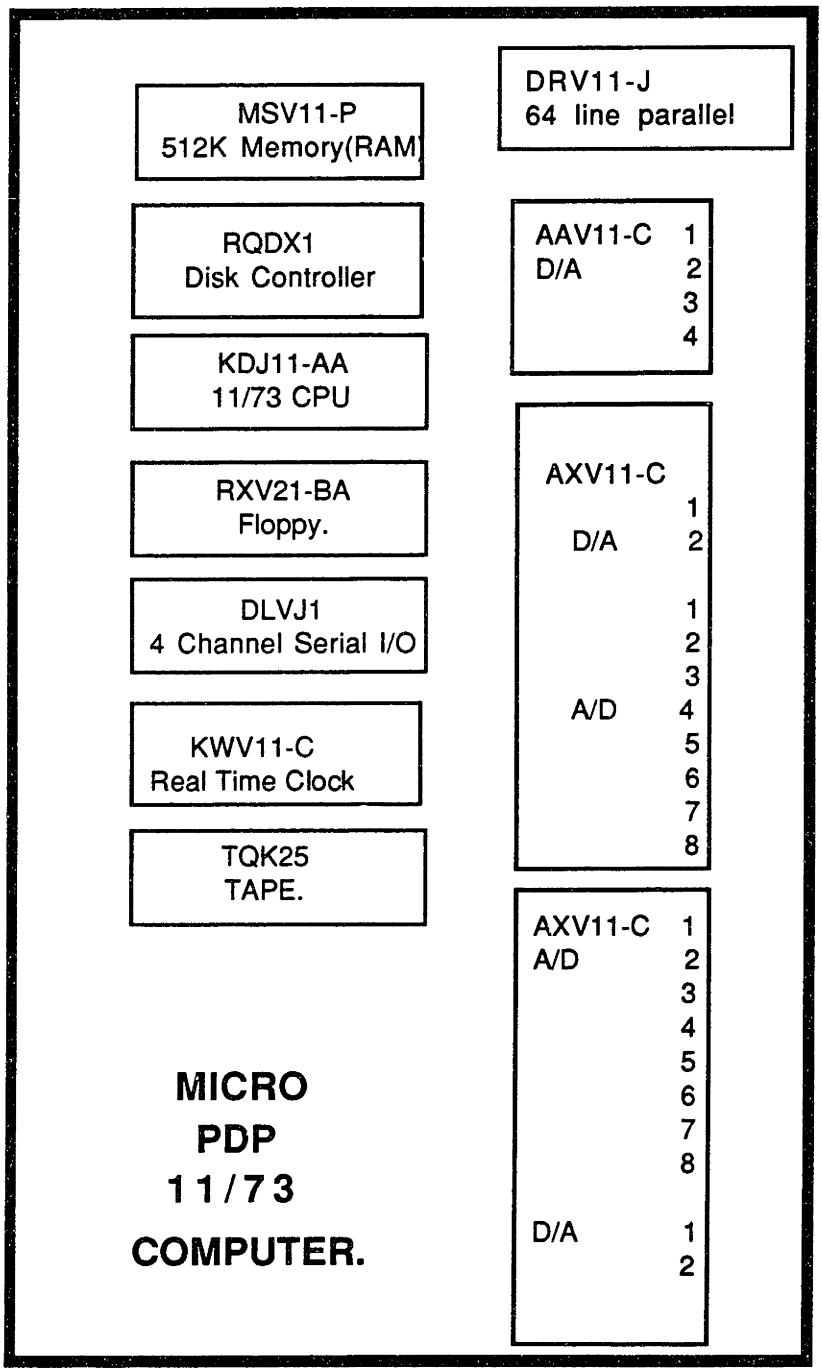

FIGURE 4-11

Computer and Relevant Boards

4.6 HARDWARE ASSEMBLY AND CONFIGURATION

The hardware was assembled having six legs, each leg being a hydraulic cylinder with its own servovalve and potentiometer mounted on it. The servovalves, force sensor and the potentiometers were linked to the PDP 11/73 computer system through the A/D and D/A boards. Commands from the computer to the platform and the robot is sent through the servocontroller. The schematic setup of the system is shown in Figure 4-12. The completed hardware is shown in Figure 4-13.

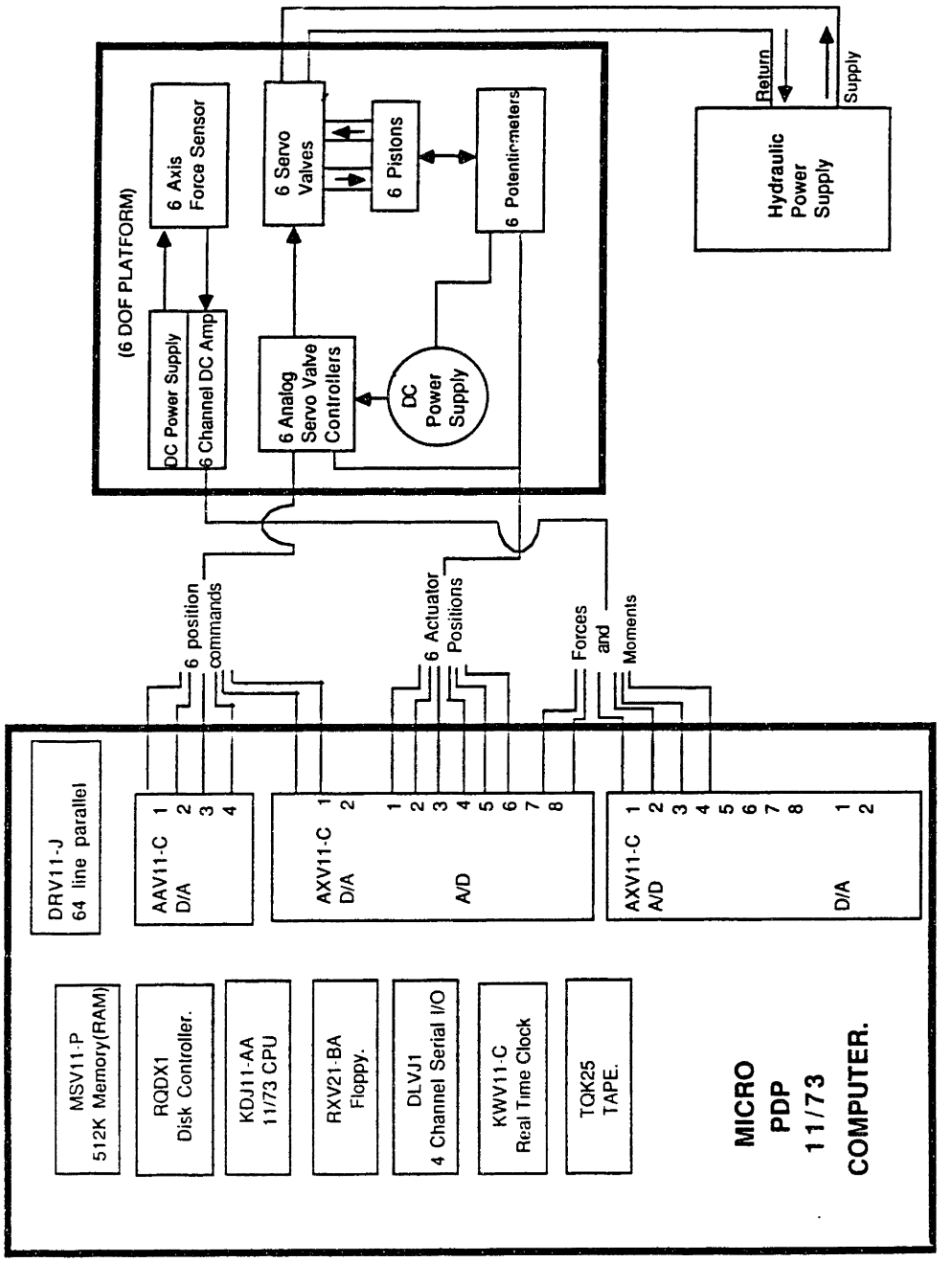

FIGURE 4-12

Schematic of the Complete System

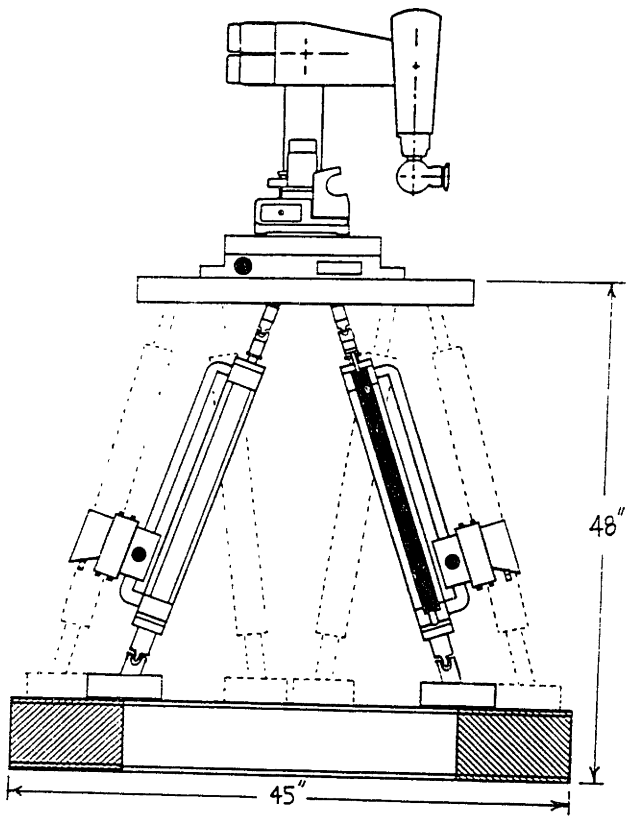

FIGURE 4-13

Completed Hardware

CHAPTER 5

KINEMATIC ANALYSIS

5.1 FORWARD AND INVERSE KINEMATICS

There are two mappings which characterize the geometry of a manipulator. In order to translate reference frame commands into the language of the manipulator, and to investigate the dynamic behavior of the system, the two mappings must either be found in closed form or synthesized by computer search. These mappings, known as the forward and inverse kinematics, relate the natural coordinates of the manipulator to reference, or absolute coordinates. The forward kinematics transform actuator coordinates into the reference coordinates of the end effector; this map tells you where you are if the stroke of each actuator is known. The inverse mapping says what should be the stroke of each actuator to reach a given position. Interestingly, the nature of the kinematic analysis of the parallel linkage is in many respects the dual of that of the serial configuration [12], [13].

For a serial arm with N links, the natural coordinates are the set of joint angles:

$$\underline{\theta} = \{ \theta_1 , \theta_2 , ... , \theta_n \}$$

which are directly determined by actuator position. Hence the forward kinematics is the mapping:

$$F : \underline{\theta} \dashrightarrow \underline{X}$$

where X represents the position of the end effector. This representation depends on the choice of reference coordinates.

In cartesian form, using Euler angles to specify orientation,

$$X = \{ x , y , z , \varphi , \psi , \theta \}$$

The inverse mapping is:

$$G : \underline{X} \dashrightarrow \underline{\theta}$$

The forward map F is a straightforward series of linear operations involving matrix transformation to account for link rotation, and vector addition to specify the position of consecutive joints. N iterations of this process yields the position of the end effector at the end of the chain. The inverse map G, determining joint angles from position, is less straightforward. For a general serial linkage the map G cannot be specified in closed form, but only approximated by a search algorithm implemented on computer. The map is plagued by singular points which may have multiple solutions or none at all. An exception to this occurs when all rotational axes are either parallel or intersect each other [14].

The natural coordinates for the parallel linkage are the link lengths, see Figure 5-1:

$$L = \{ L_1 , L_2 , \ldots\ldots , L_6 \}$$

will be used to denote the six actuator strokes. The kinematics of this configuration are the dual of the serial in that here it is the forward map

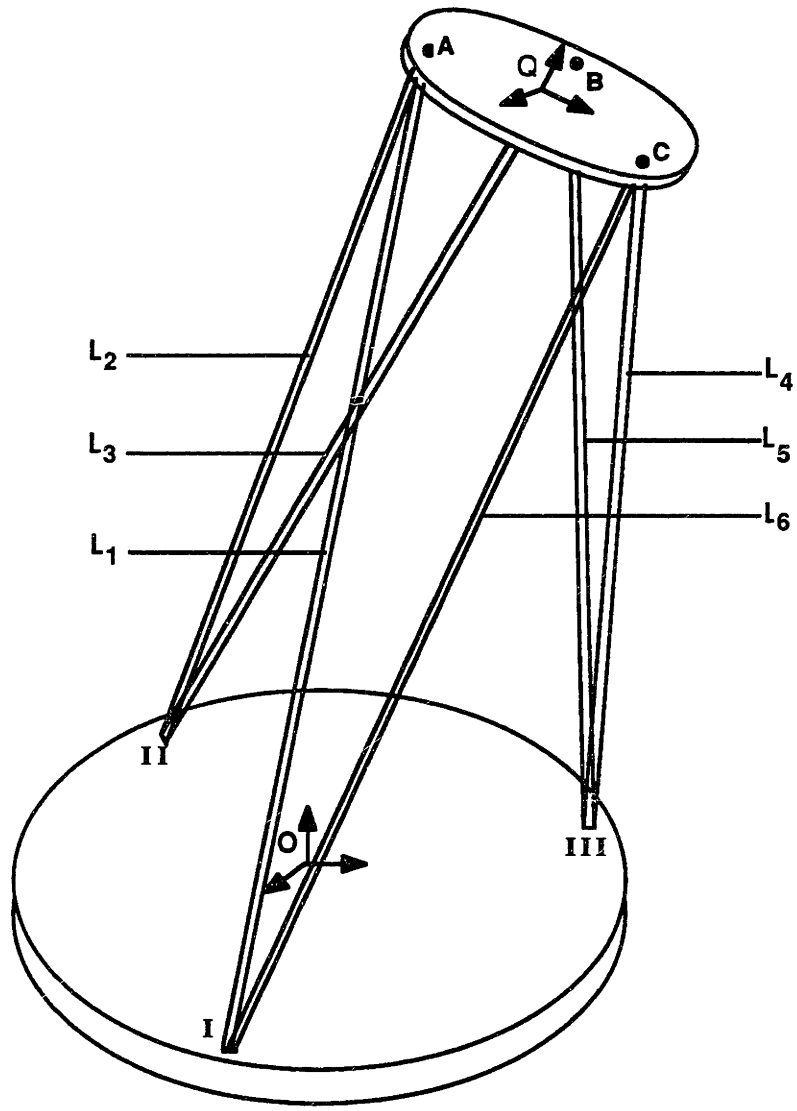

FIGURE 5-1

Parallel Linkage Mechanism

which is not closed, while the inverse is straight forward arithmetic. Both mappings are outlined in the following sections, beginning with the idealized inverse kinematics.[1]

First, some notation must be introduced. Let $\underline{X}$ be given in Spherical-Eulerian coordinates

$$X = \{ r, \alpha, \beta, \varphi, \theta, \psi \}$$

This representation lends itself naturally to the working envelope of the manipulator, which is a conical section between two concentric spherical shells, Figure 5-2. Coordinates r, α , β specify the position of the midpoint Q of the upper plate, while φ , θ , ψ are the Euler angles describing the orientation of a coordinate frame Qxyz rigidly attached to this plane. Let OXYZ be the global, inertial reference frame, with origin O at the base midpoint, see Figure 5-3.

The links in this ideal model originate at three points I, II, III on the base and connect to the upper plate at A, B, C. All points of connection behave as spherical joints, allowing the links to pivot and twist freely. In the physical system these links are hydraulic cylinders and they pivot freely on joints at top and base plates.

5.2 PARALLEL INVERSE KINEMATICS

The inverse mapping is:

---

[1]For simplicity, the discussion concerns an idealized model where the six links terminate in pairs at the three points on the base and upper plate. Accounting for the actual separation involves a little additional arithmetic and was considered in the actual implementation of the kinematic analysis.

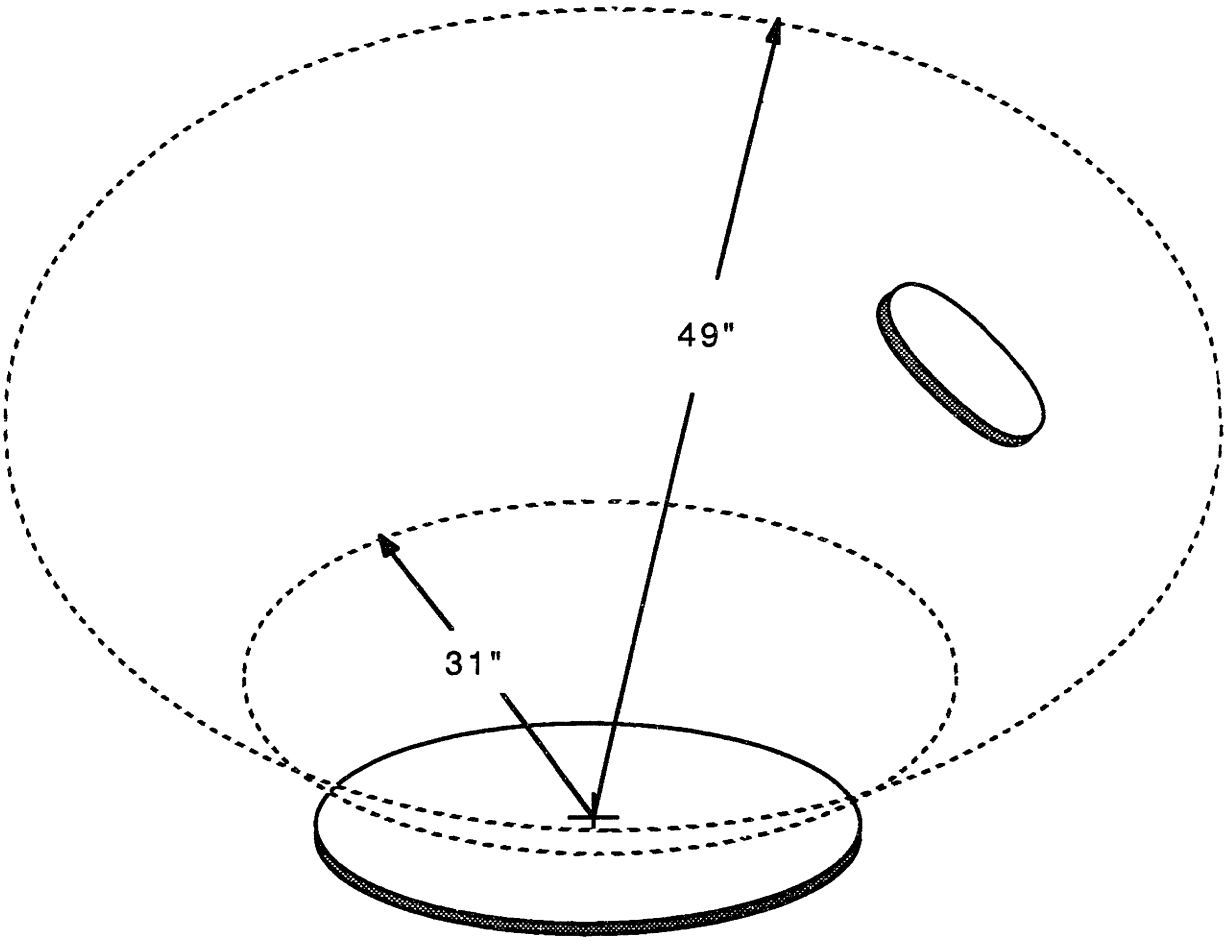

FIGURE 5-2

Conical Workspace Of Manipulator

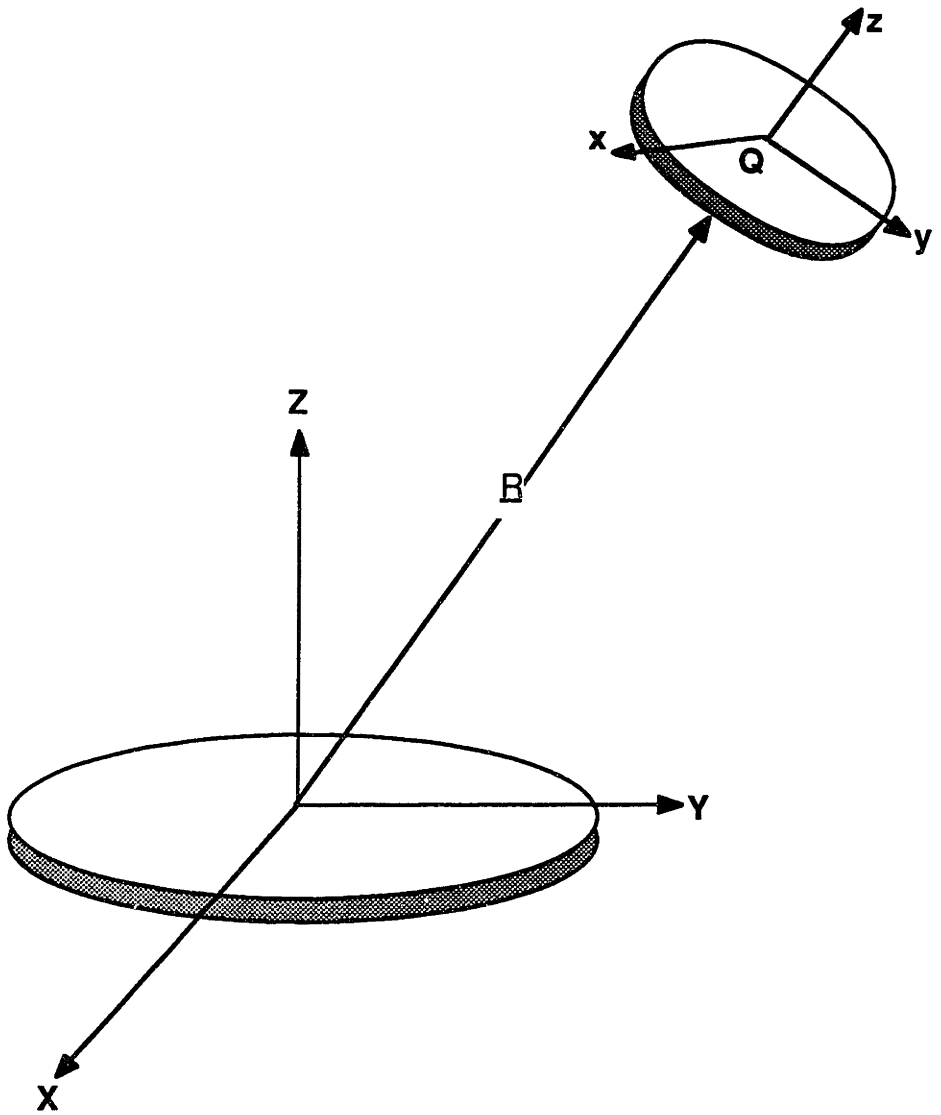

FIGURE 5-3

Reference Frames

$$G : \underline{X} \dashrightarrow \underline{L}$$

$$G = \{ G_1 , G_2 , \ldots . , G_n \} \quad \text{where} \quad G_i (X) = L_i$$

The following is an outline of the inverse kinematics for the parallel linkage, whereby the hydraulic cylinder strokes required to achieve a given position are calculated. The simplicity and speed of this algorithm are the principal advantages to the parallel geometry.

(1) Given a command position $\underline{X}$, form the Euler rotational transformation $T_{\psi\theta\varphi}$ which describes the orientation of the top plate fixed reference frame Qxyz.

(2) Compute the top plate vertex vectors $\underline{A}$, $\underline{B}$, $\underline{C}$:

$$\begin{aligned} \underline{A} &= \underline{T} * \underline{QA} + \underline{Q} \\ \underline{B} &= \underline{T} * \underline{QB} + \underline{Q} \\ \underline{C} &= \underline{T} * \underline{QC} + \underline{Q} \end{aligned} \qquad (5.1)$$

where, e.g., $\underline{QA}$ is the constant vector, expressed in coordinates Qxyz, connecting the plate midpoint Q to vertex A.

(3) Calculate the six cylinder strokes

$$\begin{aligned} L_1 &= | \underline{A} - \underline{I} | \\ L_2 &= | \underline{A} - \underline{II} | \\ L_3 &= | \underline{B} - \underline{II} | \\ L_4 &= | \underline{B} - \underline{III} | \\ L_5 &= | \underline{C} - \underline{I} | \\ L_6 &= | \underline{C} - \underline{III} | \end{aligned} \qquad (5.2)$$

5.3 PARALLEL FORWARD KINEMATICS

The forward mapping is defined as

$$F : \underline{L} \dashrightarrow \underline{X}$$

The forward mapping from link lengths to position are neither globally well behaved nor defined. Indeed, it is not obvious that the six link lengths $\underline{L}$ uniquely determine the position of the plate. Grubler's criterion suggests that, at least locally, the linkage is rigid:

Number of D.O.F - six[1]

$= 6 * (n - 1) - 3 * P - 6$ " P " for pinned (ball) joints

$= 6 * (8 - 1) - 3 * 12 - 6$

$= 0$

Local rigidity, however, does not imply global uniqueness; multiple solutions $\underline{X}$ corresponding to a given $\underline{L}$ are possible. Two further mathematical constraints are necessary to ensure uniqueness:

(1) The z - coordinate of the end effector is positive (Upper plate must be above the base).

(2) The scalar product between the radius vector OQ and upper plate normal n must be positive (top plate cannot pivot so far as to hit the actuators, its normal can be inclined at most 90^o to the imaginary line connecting the center points of the top and base plates).

---

[1]Subtracting the degrees of freedom corresponding to twist in each link about its centerline, which is of no consequence to plate position.

Note that both of these criteria are also physical constraints on the hardware.

Before proceeding further with a practical description of the forward kinematics, a purely mathematical observation concerning this mapping as the inverse of map G provides some useful insight. Consider a state $\underline{X}_o$ of our system where the Jacobian determinant is non-vanishing:

$$\left| J \right|_{\underline{X}_o} = \begin{vmatrix} \frac{\partial G_1}{\partial r} & \frac{\partial G_1}{\partial \alpha} & \cdots & \frac{\partial G_1}{\partial \phi} \\ \frac{\partial G_2}{\partial r} & \frac{\partial G_2}{\partial \alpha} & \cdots & \frac{\partial G_2}{\partial \phi} \\ \cdot & & & \\ \cdot & & & \\ \cdot & & & \\ \frac{\partial G_6}{\partial r} & \frac{\partial G_6}{\partial \alpha} & \cdots & \frac{\partial G_6}{\partial \phi} \end{vmatrix} \neq 0$$

Then the fundamental inverse function theorem guarantees the existence of a continuously differentiable inverse $F = G^{-1}$ in some neighborhood W about $\underline{L}_o = G\{\underline{X}_o\}$.

This guarantees the local existence and differentiability of F, the forward kinematics, in some neighborhood of a non-singular state. This also shows that locally, the six links L_i may be independently specified.

5.4 IMPLEMENTATION OF FORWARD KINEMATICS

Practically, the solution of the forward kinematics involves solving a set of simultaneous quadratic equations (Equation 5.2) together with the

constraint equations. These specify that the upper tie points A, B, C are vertices of an equilateral triangle of side p:

$$| \underline{A} - \underline{B} | = | \underline{A} - \underline{C} | = | \underline{B} - \underline{C} | = p \qquad (5.3)$$

Two techniques were considered for determining the position $\underline{X}$ of the top plate from the hydraulic cylinder strokes L. The first is a direct integration:

$$\text{Given } \underline{dL} = J * \underline{dX}$$

$$\underline{dX} = J^{-1} * \underline{dL}$$

$$\text{Hence } X = \int_{\underline{L_o}}^{\underline{L}} J^{-1} * \underline{dL} \quad + \quad \underline{X_o}$$

The position may thereby be estimated to high accuracy, but at the expense of successively calculating J^{-1}.

The second method is a search based on a geometrical interpretation of equations (5.2) and (5.3). The following approach based on the geometry of the platform was investigated and is outlined below.

The theory behind this approach is that the equations (5.2) describe six spheres of radius L_i, centered two each at the fixed base vertices I, II, III. Intersecting these spheres yields three circles whose centers are on lines containing the base triangle I, II, III and which lie in planes perpendicular to these lines. The upper plate must be positioned with each vertex lying on the corresponding circle, see Figure 5-4. This position will be $\underline{X}$, the kinematic inversion of $\underline{L}$. The strategy to find this position is to form a

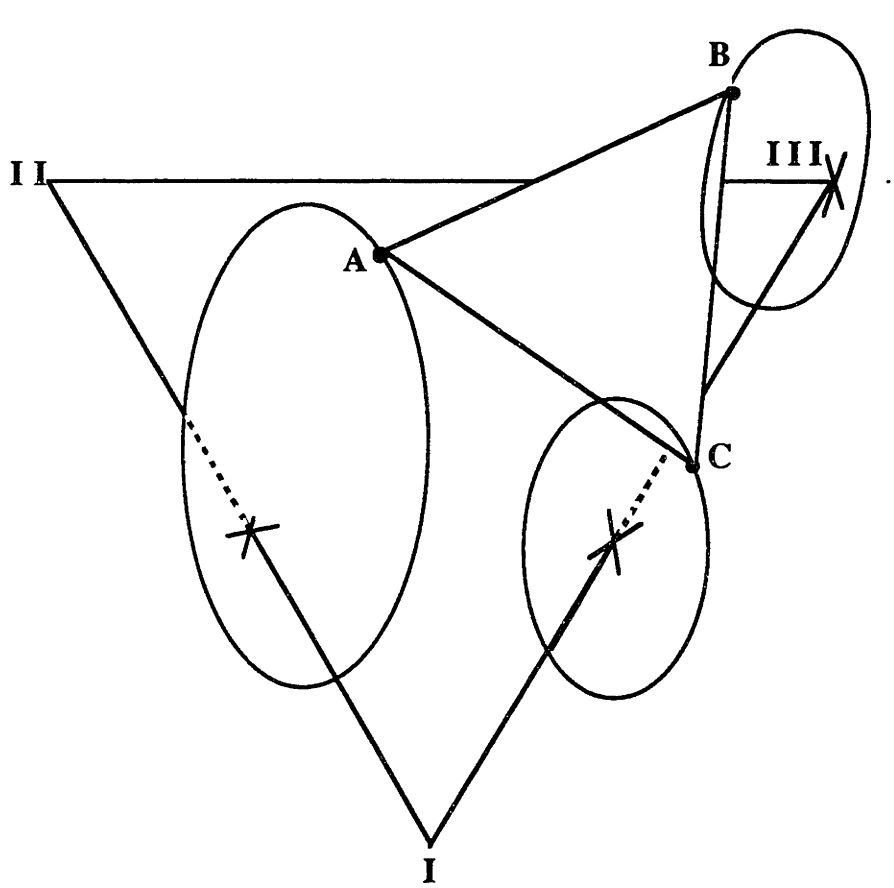

FIGURE 5-4

Forward Kinematics Search

sphere of radius P with center Q on one of the circles, and observe the distance between intersection points of this sphere with the other two circles as Q moves along the first. There may be two, one or no point of intersection with each. A candidate solution is found when the intersection points are a distance p apart, for then the center Q will form an equilateral triangle with each of the two intersection points. Note that the candidate solution, though satisfying the constraint equations, is not necessarily physically possible, e.g. to each $\underline{X}$ there corresponds a mirror solution with the plate underneath the base. In addition to multiple roots is the possibility of no solution at all, e.g. for

$$L_1 > L_2 + s$$

where s is the separation of base points I, II. Generally, if the initial guess is in the neighborhood of a physical solution (e.g. the last position of the manipulator) then the algorithm quickly converges to a unique, realizable solution.

In order to fully apply this method to our system we also need to consider the separation distance between the joints at the top and the bottom plate. In this case we will have six joints at the bottom and six joint at the top. Since all the base joints are fixed therefore the motion of the upper plate of platform is dependent only on the different configuration of the top six joints. Each top joint movement is restricted in three directions by the adjacent top joint on each side and the base joint to which it is connected by the actuator. Hence each of these top joints will act as a center of three spheres and radius of these spheres will be equal to the distance to the joints which affects its motion [15]. Obviously some parts of these three spheres for

each top joint will be overlapping each other and the intersection of these spheres is the workspace of that top joint. The terminology used in formulating the kinematic equations is shown in Figure 5-5, where

L_i = Cylinder stroke + length of cylinder ; i = 1,2, ... ,6

A_i = Base joints ; i = 1,2, ... ,6

A_i = Top joints ; i = 7,8, ... ,12

$L_{i,k}$ = Distance between joint i and k

R = Radius of bottom plate

r = Radius of top plate

Now we can write a set of 18 simultaneous quadratic equations which are non-linear in nature [15]. The following six equations relate the top U-joints to the base U-joints by the sphere equation using the instantaneous length of the cylinder as the radius:

$$(X_{A1} - X_{A7})^2 + (Y_{A1} - Y_{A7})^2 + (Z_{A1} - Z_{A7})^2 = L_1^2 \qquad (5.4)$$

$$(X_{A2} - X_{A8})^2 + (Y_{A2} - Y_{A8})^2 + (Z_{A2} - Z_{A8})^2 = L_2^2 \qquad (5.5)$$

$$(X_{A3} - X_{A9})^2 + (Y_{A3} - Y_{A9})^2 + (Z_{A3} - Z_{A9})^2 = L_3^2 \qquad (5.6)$$

$$(X_{A4} - X_{A10})^2 + (Y_{A4} - Y_{A10})^2 + (Z_{A4} - Z_{A10})^2 = L_4^2 \qquad (5.7)$$

$$(X_{A5} - X_{A11})^2 + (Y_{A5} - Y_{A11})^2 + (Z_{A5} - Z_{A11})^2 = L_5^2 \qquad (5.8)$$

$$(X_{A6} - X_{A12})^2 + (Y_{A6} - Y_{A12})^2 + (Z_{A6} - Z_{A12})^2 = L_6^2 \qquad (5.9)$$

The following six sphere equations relate the top plate's odd and even joints:

$$(X_{A7} - X_{A8})^2 + (Y_{A7} - Y_{A8})^2 + (Z_{A7} - Z_{A8})^2 = L_{7,8}^2 \qquad (5.10)$$

$$(X_{A8} - X_{A9})^2 + (Y_{A8} - Y_{A9})^2 + (Z_{A8} - Z_{A9})^2 = L_{8,9}^2 \qquad (5.11)$$

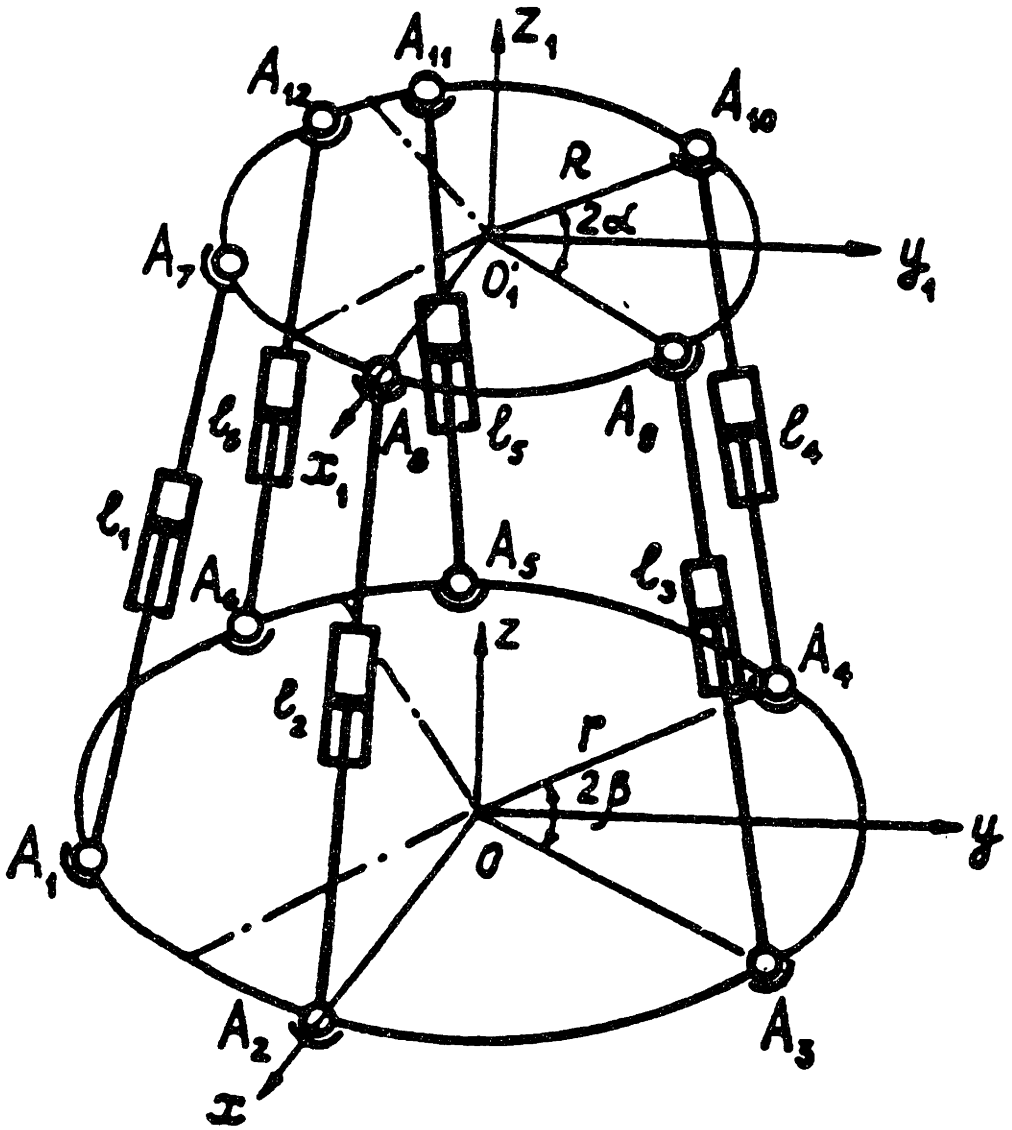

FIGURE 5-5

Stewart Platform Terminology

$$(X_{A9} - X_{A10})^2 + (Y_{A9} - Y_{A10})^2 + (Z_{A9} - Z_{A10})^2 = L_{9,10}^2 \quad (5.12)$$

$$(X_{A10} - X_{A11})^2 + (Y_{A10} - Y_{A11})^2 + (Z_{A10} - Z_{A11})^2 = L_{10,11}^2 \quad (5.13)$$

$$(X_{A11} - X_{A12})^2 + (Y_{A11} - Y_{A12})^2 + (Z_{A11} - Z_{A12})^2 = L_{11,12}^2 \quad (5.14)$$

$$(X_{A7} - X_{A12})^2 + (Y_{A7} - Y_{A12})^2 + (Z_{A7} - Z_{A12})^2 = L_{7,12}^2 \quad (5.15)$$

The following six sphere equations relate the top plate's alternate joints:

$$(X_{A7} - X_{A9})^2 + (Y_{A7} - Y_{A9})^2 + (Z_{A7} - Z_{A9})^2 = L_{7,9}^2 \quad (5.16)$$

$$(X_{A9} - X_{A11})^2 + (Y_{A9} - Y_{A11})^2 + (Z_{A9} - Z_{A11})^2 = L_{9,11}^2 \quad (5.17)$$

$$(X_{A7} - X_{A11})^2 + (Y_{A7} - Y_{A11})^2 + (Z_{A7} - Z_{A11})^2 = L_{7,11}^2 \quad (5.18)$$

$$(X_{A8} - X_{A10})^2 + (Y_{A8} - Y_{A10})^2 + (Z_{A8} - Z_{A10})^2 = L_{8,10}^2 \quad (5.19)$$

$$(X_{A10} - X_{A12})^2 + (Y_{A10} - Y_{A12})^2 + (Z_{A10} - Z_{A12})^2 = L_{10,12}^2 \quad (5.20)$$

$$(X_{A8} - X_{A12})^2 + (Y_{A8} - Y_{A12})^2 + (Z_{A8} - Z_{A12})^2 = L_{8,12}^2 \quad (5.21)$$

The above equations are nonlinear in nature, hence a closed form solution is not possible. they can be solved by using suitable numerical methods. The procedure used was known as Multidimensional Newton-Raphson method. Newton-Raphson method is dependent on an initial guess. It converges very fast to a unique, realizable solution if the initial guess is in the vicinity of a physical solution, depending on the degree of accuracy required. Basically, it is an iterative process and can be defined as

$$X_{n+1} = X_n - \frac{f(X_n)}{f'(X_n)} \quad (5.22)$$

A computer can be programmed with feedback to keep repeating the process of equation (5.22), as indicated in Figure 5-6.

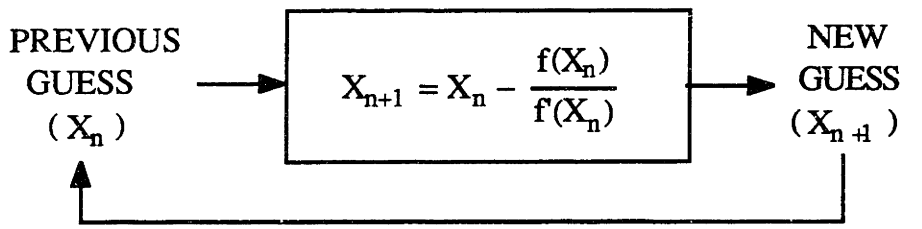

FIGURE 5-6

Feedback for Iterating using Newton's method

For equations (5.4) to (5.21), the values of the base joints location were actually measured from the physical system and are as followed:

JOINTS	X	Y	Z
A_1	15.8939	9.1441	0
A_2	0	18.2950	0
A_3	-15.7157	9.3157	0
A_4	-15.8768	-9.2349	0
A_5	0	-18.2950	0
A_6	15.8776	-8.8766	0

The separation distance between the top joints were measured from the actual physical system and are given below:

$L_{7,8}$ = 6.7983" $L_{8,9}$ = 14.7208"

$L_{9,10}$ = 6.7983" $L_{10,11}$ = 14.7208"

$L_{11,12}$ = 6.7983" $L_{7,12}$ = 14.7208"

$L_{7,9}$ = 19.0525" $L_{9,11}$ = 19.0525"

$L_{7,11}$ = 19.0525" $L_{8,10}$ = 19.0525"

$L_{10,12}$ = 19.0525" $L_{8,12}$ = 19.0525"

The computer program was written in FORTRAN language and implemented on DIGITAL MICROVAX computer. Generally, forward mapping is locally well behaved. The only problem is that, in order to solve forward kinematics for any physical position, we have to input a search seed, or initial guess, in the neighborhood of the physical solution. This limits the usefulness of this method. Ideally, we would have preferred a method which is independent of an initial guess, but the nonlinear nature of the simultaneous quadratic equations prohibit it.

The second alternative is to have one standard initial guess which can be used to locate all the physical positions in the specified workspace of platform with reasonable accuracy. The approach used involve solving the inverse kinematics of the system. In this method, using any feasible initial guess, an initial solution to the physical position for the given instantaneous length of the actuators is obtained through the forward kinematics. This solution is then used in solving the inverse kinematics to obtain a set of hydraulic cylinder stroke values. These stroke values are then compared with the actual stroke values for error. If the error is more than the required accuracy, the previous solution of the forward kinematics is then

used as the second initial guess for the forward mapping. This method is repeated until a generalized value of initial guess is obtained which satisfy all the physical positions inside the specified workspace. This learning process needs to be solved only once for any given workspace. The values of standard initial guess obtained for our system are:

JOINTS	X	Y	Z
A_7	8.029702	7.332339	39.17744
A_8	2.141053	10.729471	39.21962
A_9	-10.605020	-3.364681	39.22329
A_{10}	-10.602661	-3.433694	39.22409
A_{11}	2.148515	-10.789642	39.23077
A_{12}	8.034839	-7.388477	39.19537

The above values can be used as a standard initial guess for Newton-Raphson method to solve the forward kinematics for all the positions in the workspace of our platform. Forward kinematics solved by using the above generalized guess locates any permissible physical position within four digits of accuracy Hence, we overcome the problem of inputting a new guess value for each new position. The above values can be made an integral part of a computer program used to solve the forward kinematics. The computer program will now need only the actuator stroke values to determine the position of the top plate of the platform at any instant of time.

Of the two mappings, forward and inverse, it is the inverse kinematics which must be computed on-line for real time trajectory control of the

platform. Hence the tremendous computational advantage of the parallel configuration over the serial geometry; a microprocessor will be adequate for on-line trajectory control of this manipulator. For the dynamic analysis of the manipulator, however, both forward and inverse kinematics are necessary. Forward kinematics can also be used to determine the initial position of the top plate after the start up of the system.

CHAPTER 6

SYSTEM CONTROL

6.1 CONTROL OVERVIEW

The behavior of various physical systems vary even when the external forces applied to them are similar. An instantaneous power flows between two systems that interact with each other and can be defined as the product of force and velocity. In general, physical systems can be viewed as admittance or impedance: admittances, which accept effort (force) inputs and yield flow (motion) outputs; and impedances which accept flow (motion) inputs and yield effort (force) outputs. In our case, the robot and the platform are the two physical systems that interact with each other. The platform is basically trying to simulate an environment that the robot is interacting with. Therefore, from the causality point of view, the platform is behaving as an admittance, and the robot is behaving as an impedance. So, admittance control for the platform is desired [5].

6.1.1 VARIABLE ADMITTANCE CONTROL

A variable admittance controller's action would consists of measuring the external forces on the platform and using numerical integration techniques, calculating the desired position response of the platform, and setting the command input to the position control servo equal to this calculated value. The block diagram is shown in Figure 6-1, where G(s) is the

servo system (plant) transfer function under position control and is explained in the next topic. The overall transfer function for the whole system will be the product of these two blocks.

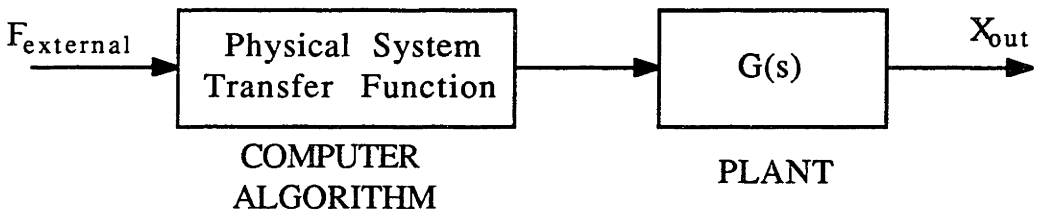

FIGURE 6-1

Admittance Control

In order to do the analysis, we consider our mechanical system to be composed of masses, springs, and dampers and we would like to obtain the equations of motion for three dimensional objects that have six degrees of freedom. Six degrees of freedom platform can be modelled by a spring-mass-damper system [5] as shown in Figure 6-2. The equations of motion obtained can be solved simultaneously by numerical integration methods in real time and hence the desired platform position can be determined. In order to simulate a space environment, all the linear and angular stiffness and damping terms of the equations of the motion are set to zero, then a case can be simulated where a robot is mounted on a spacecraft.

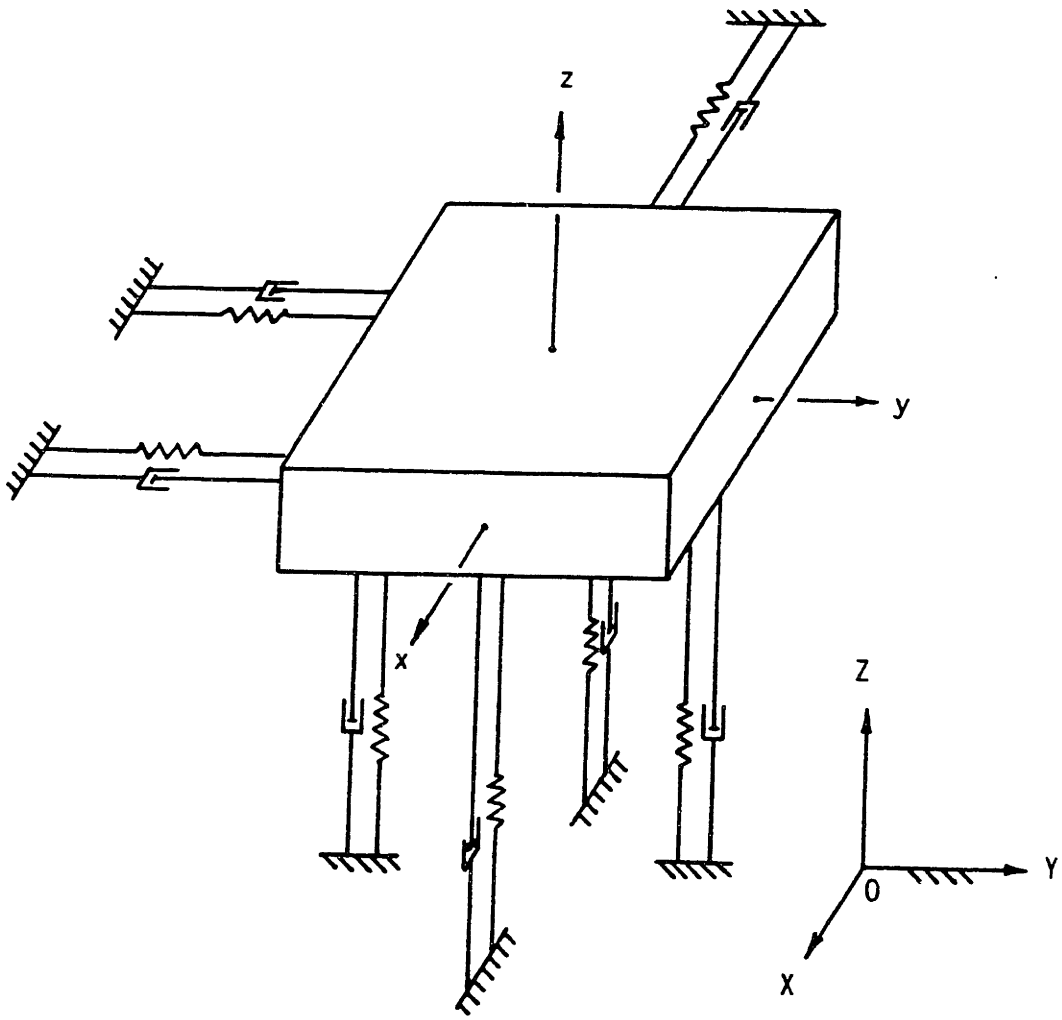

FIGURE 6-2

Admittance Model in 6 DOF

6.2 MODELLING OF SERVOVALVES

An electrohydraulic servovalve is a very complicated component to analyze. Because of the variation in valve parameters, both static and dynamic, the actual control ratio or transfer function Q(s)/I(s) [where Q(s) and I(s) are the Laplace function of flow and current, respectively] is an eighth order function. Added to this complexity are the various nonlinearities that exist within the valve, e.g. Hysteresis, spool valve friction, temperature, orifice discharge coefficient, etc. [16], [17].

As the servovalve is only one component of many in the overall servo system, taking into consideration all the variables to generate a high-order transfer function does not create a corresponding improvement in the degree of accuracy in predicting the response. Generally, for systems operating within resonances below 120 Hz (750 rad/sec), a first-order transfer function will suffice, therefore for our servovalve we assume the following first-order transfer function.

$$\frac{Q(s)}{I(s)} = \frac{K_s}{(\tau s + 1)} \qquad (6.1)$$

where $Q(s)$ is flow rate in cubic inches/sec

$I(s)$ is current in Amperes

τ is servovalve time constant in seconds

K_s is servovalve gain in cubic inches/sec/Amperes

s is Laplace operator

6.2.1 THE CLOSED LOOP POSITION CONTROL SYSTEM

The system consists of a servovalve which controls the linear position of a double-acting hydraulic cylinder, shown in Figure 6-3. The linear position of the cylinder is fed back to the controller through a linear potentiometer, hence the loop is closed. Assuming that the fluid is incompressible for the loads and operating frequencies concerned. The block diagram of the system is shown in Figure 6-4.

where K_g = Variable amplifier gain (Amps/Volts)

K_s = Servovalve gain ($inch^3/sec/Amps$)

K_p = Potentiometer sensitivity (Volts/inch)

A = Cylinder's Piston area ($inch^2$)

The transfer function of this closed loop servo system with a proportional controller is of second order, see Figure 6-5. It is given as

$$G(s) = \frac{K}{s^2 + as + K} \qquad (6.2)$$

where $G(s)$ = Transfer function of the system

a = $1/\tau$, the inverse of servovalve time constant

K = Feedforward DC gain of the closed loop system
$= \frac{K_g K_s K_p}{A\tau}$

6.2.2 EXPERIMENTAL RESULTS

The plant transfer function G(s) was experimentally determined by using a Bruel & Kjaer 3032 Dual Channel Analyzer. The analyzer compares the input signal and the output signal to the plant at different frequencies and generates the closed loop frequency response of the system [18]. The experimentally determined Bode plots of all the six actuators are shown in

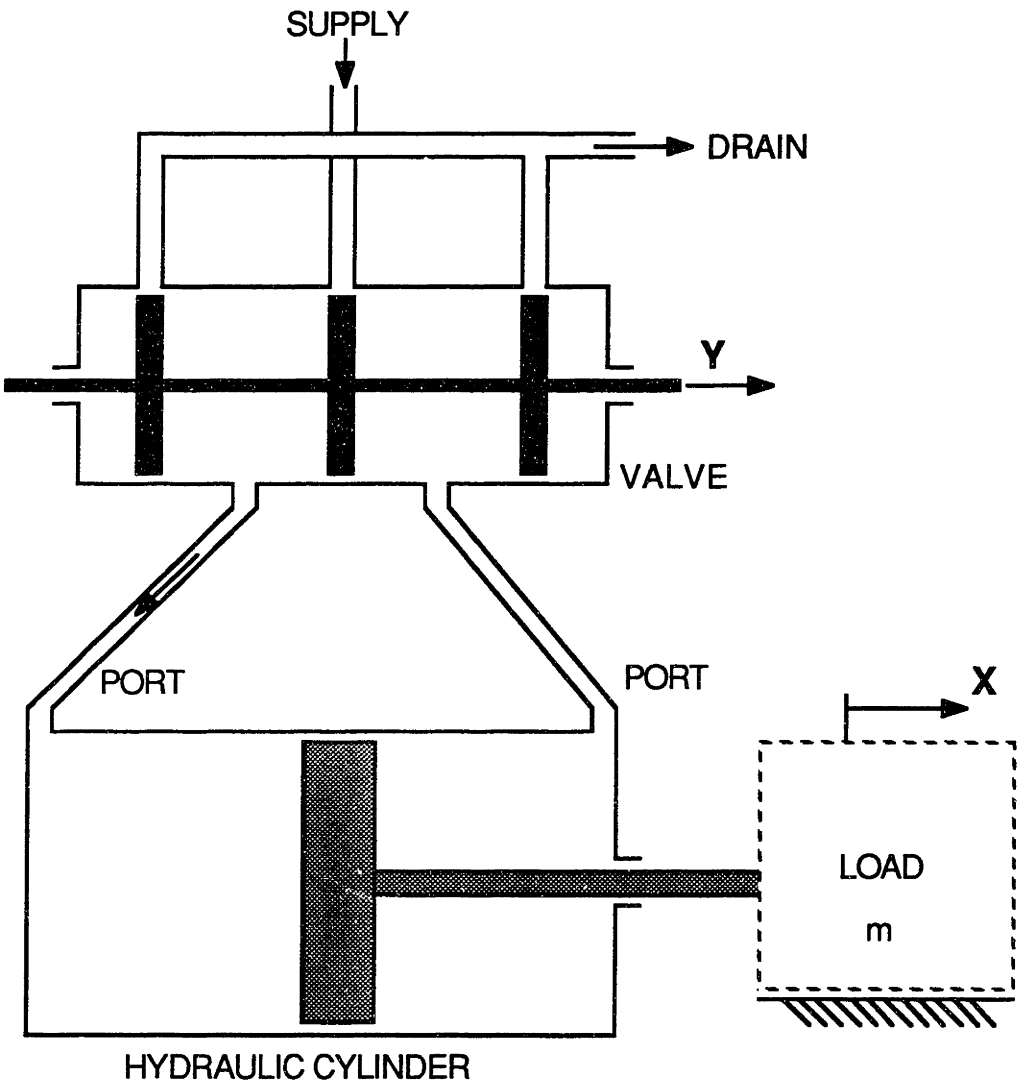

FIGURE 6-3

HYDRAULIC SERVO SYSTEM

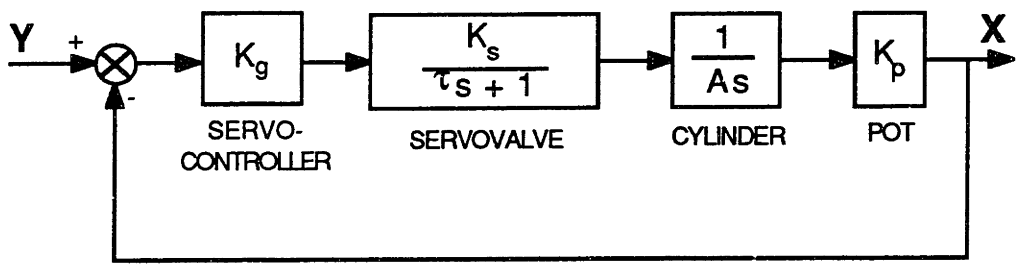

FIGURE 6-4

BLOCK DIAGRAM OF POSITION SERVO SYSTEM

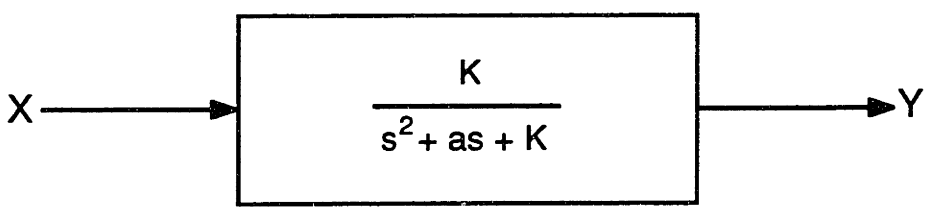

FIGURE 6-5

Equivalent Block Diagram

Figures 6-6 to 6-11. From the experimental results we see that the bandwidth of actuators is roughly 13 Hertz and hence it satisfies the design bandwidth of 5 Hertz. The order of the system is atleast two as the phase lag of the system exceeds 180 degrees.

Hence we can safely assume that the transfer function given by the equation (6.2) best approximates the closed loop servo system and our system will be structurally stable within the design operating bandwidth of 5 Hertz.

From the experimental bode plots, the parameters a and K are found out to be 38 and 3200 respectively. Hence the transfer function of the plant can be given as

$$G(s) = \frac{3200}{s^2 + 38s + 3200} \qquad (6.3)$$

The Bode plot of the estimated transfer function is shown in Figure 6-12. Both Phase margin and Gain margin are positive, indicating that the system is stable.

The unit step response of the underdamped system is shown in Figure 6-13. The transient response characteristics of the system to a unit step input are given below:

Rise time = 0.0358 sec

Peak time = 0.059 sec

Maximum overshoot= 33%

Settling time = 0.2 sec for 2% criterion

Although the maximum overshoot is little high but the settling time of the system response is very fast, hence quickly closing on the command

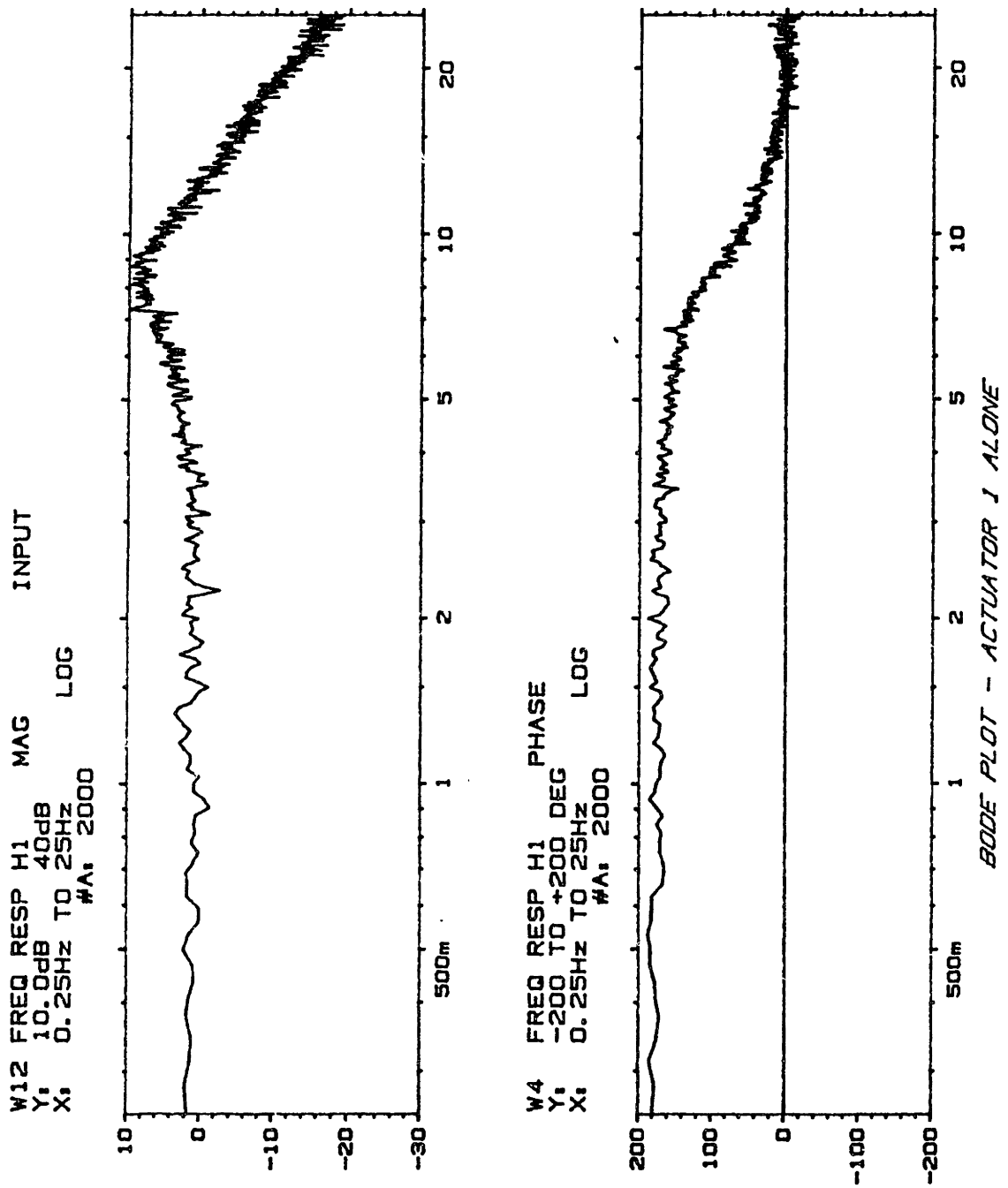

Figure 6-6

Experimental Bode Plot For Actuator 1

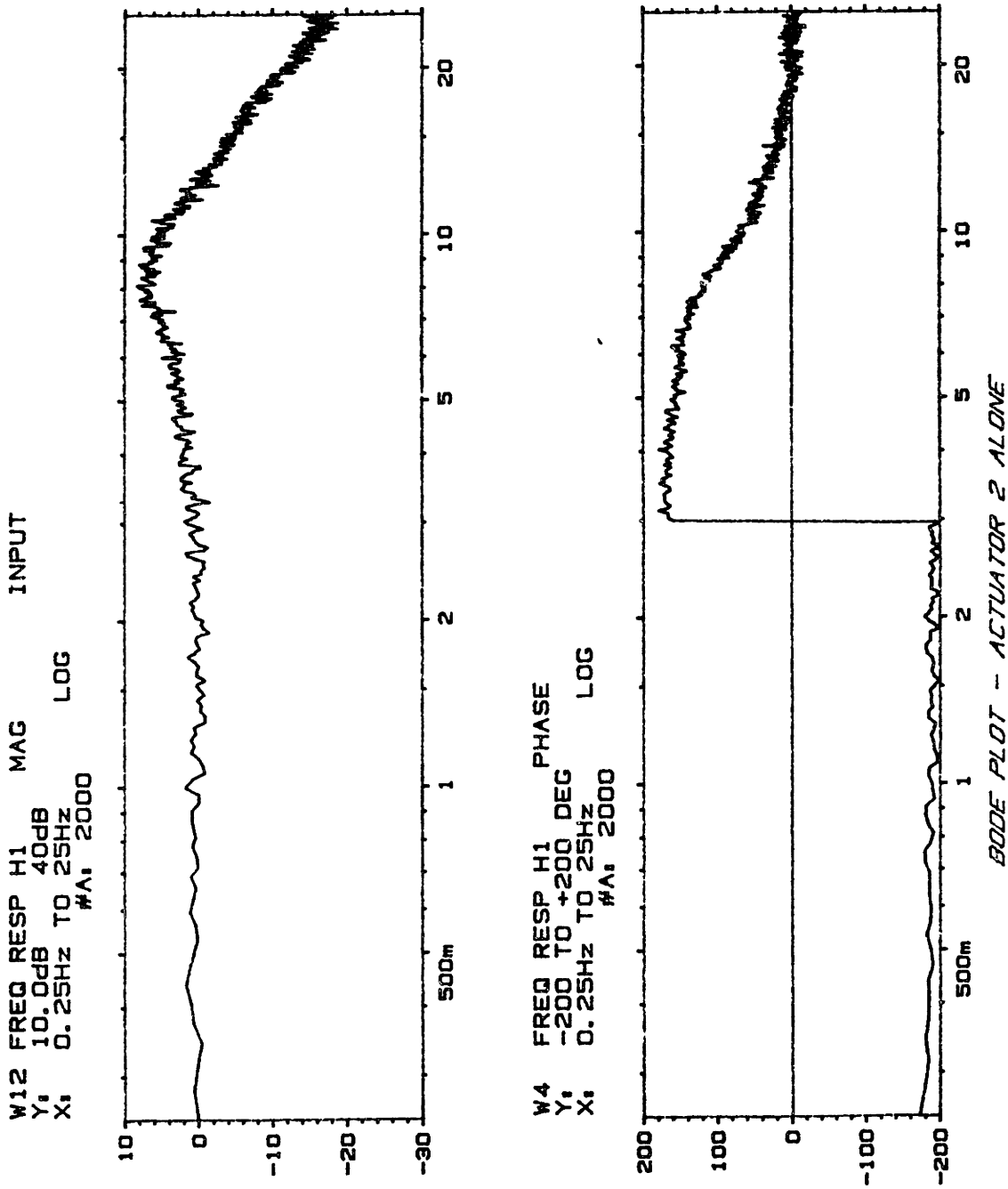

Figure 6-7

Experimental Bode Plot For Actuator 2

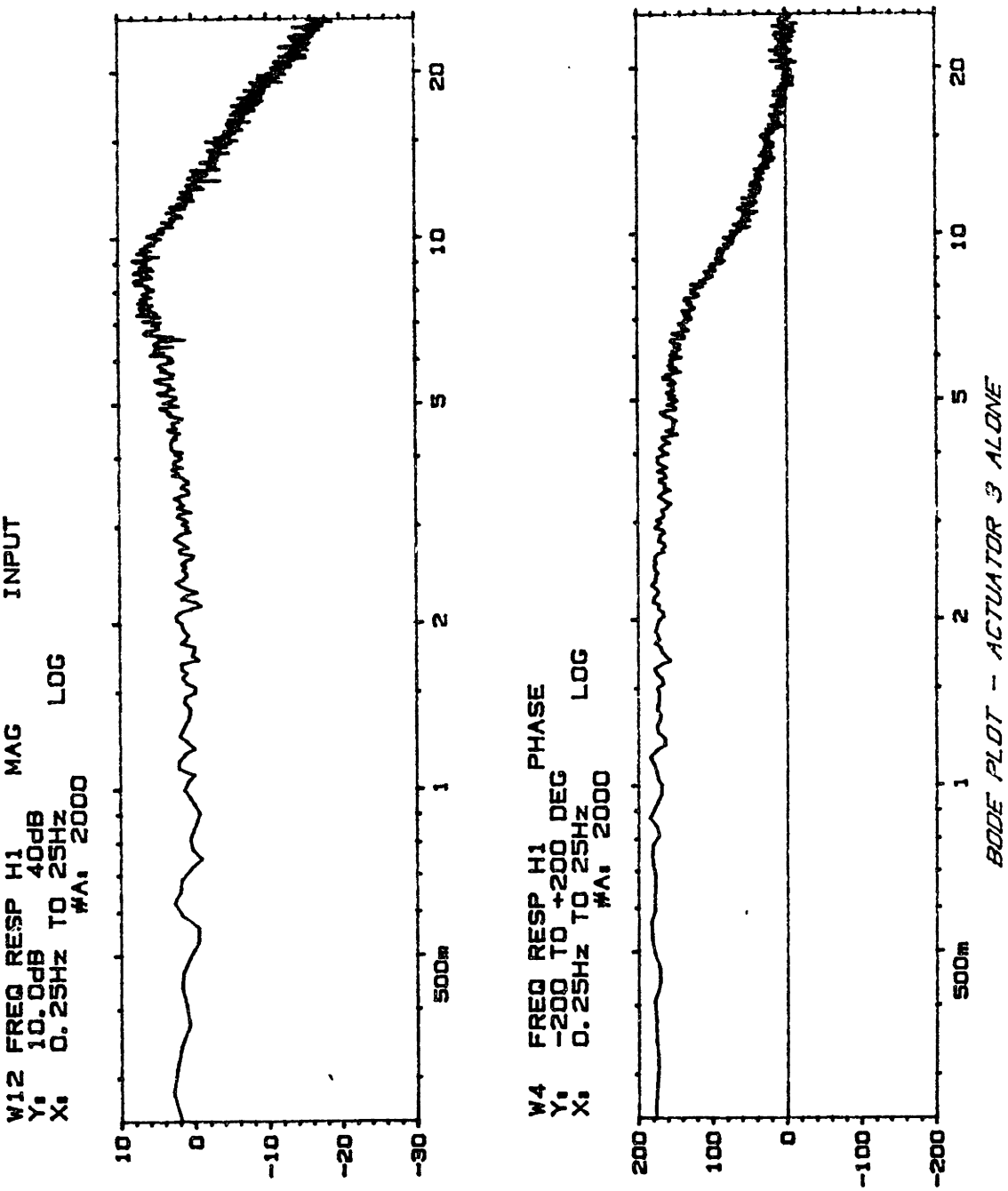

Figure 6-8

Experimental Bode Plot For Actuator 3

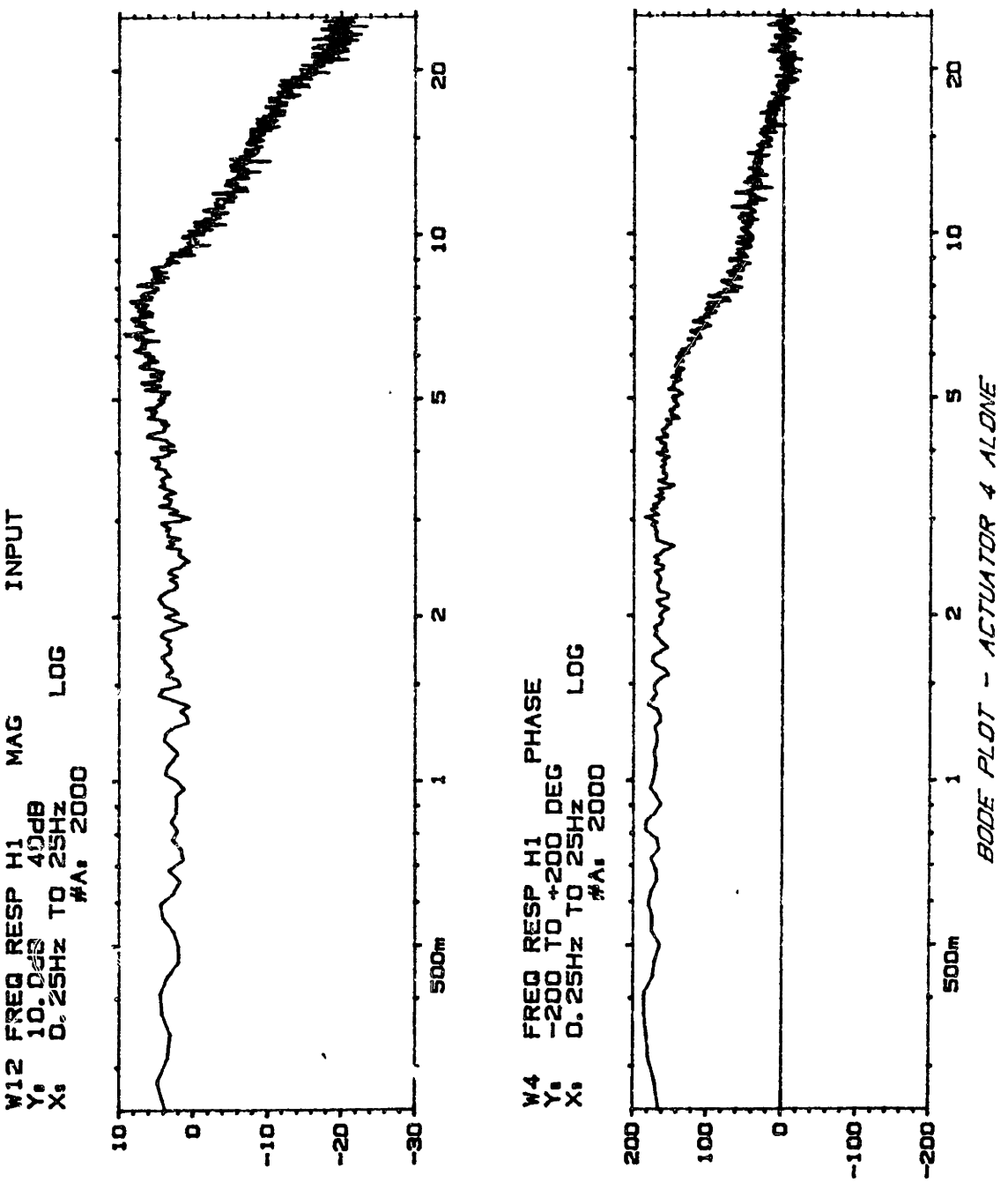

Figure 6-9

Experimental Bode Plot For Actuator 4

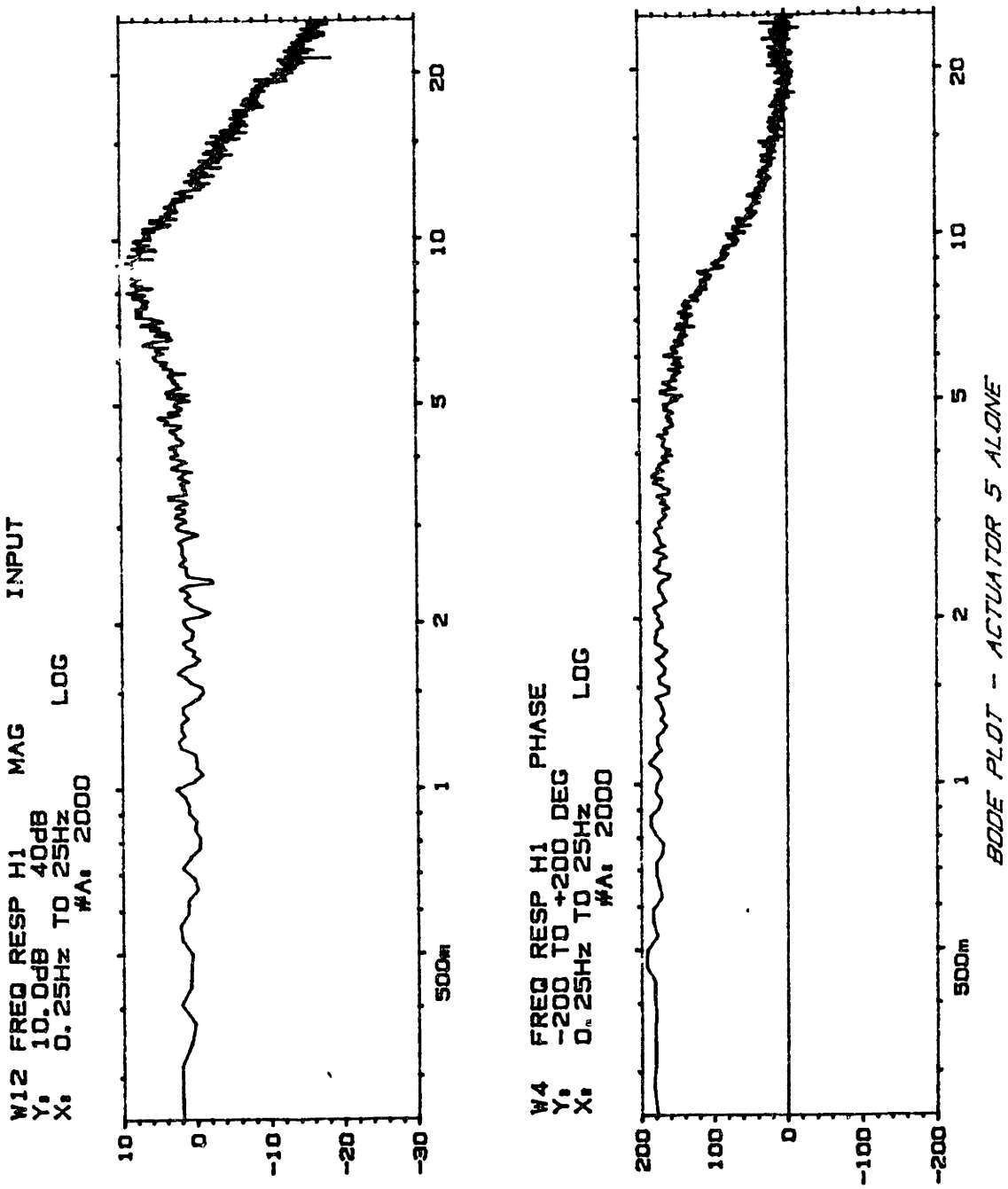

Figure 6-10

Experimental Bode Plot For Actuator 5

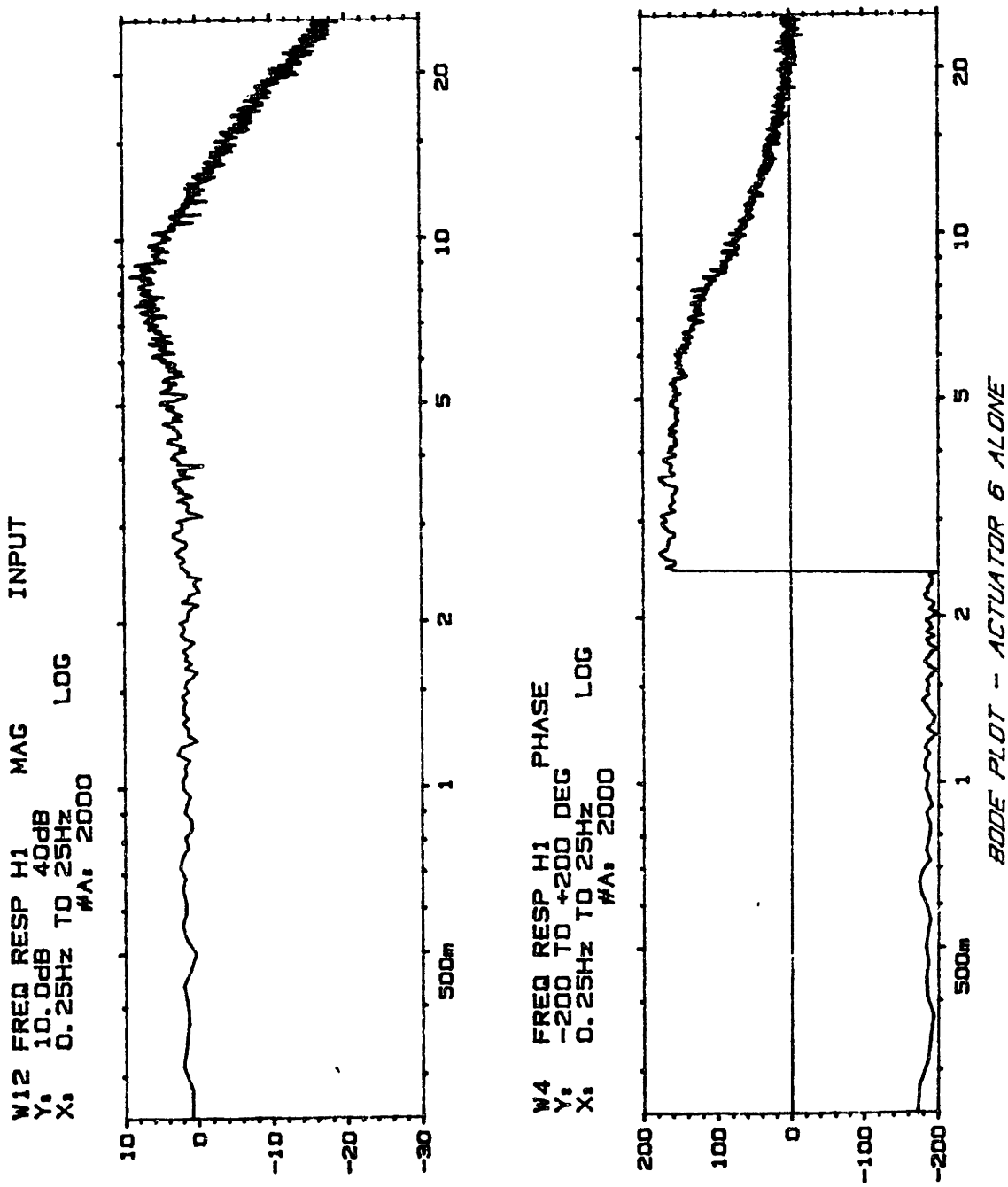

Figure 6-11

Experimental Bode Plot For Actuator 6

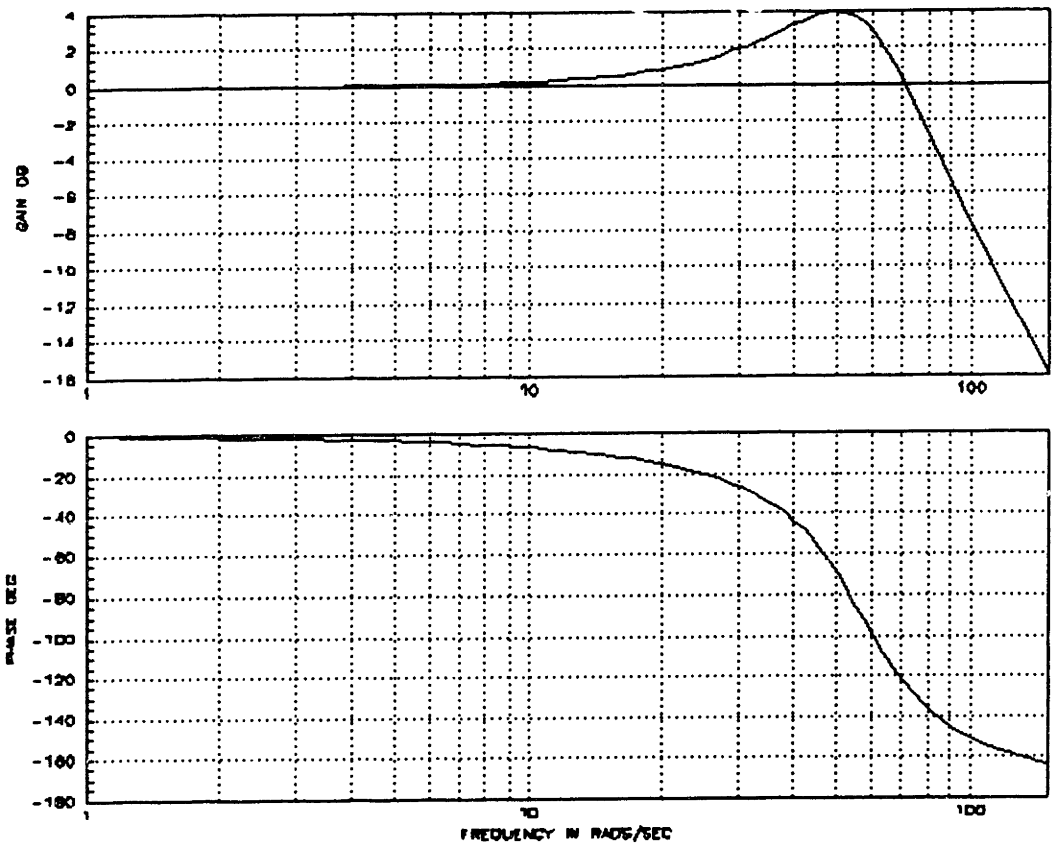

Figure 6-12

Bode Plot For The Estimated G(s)

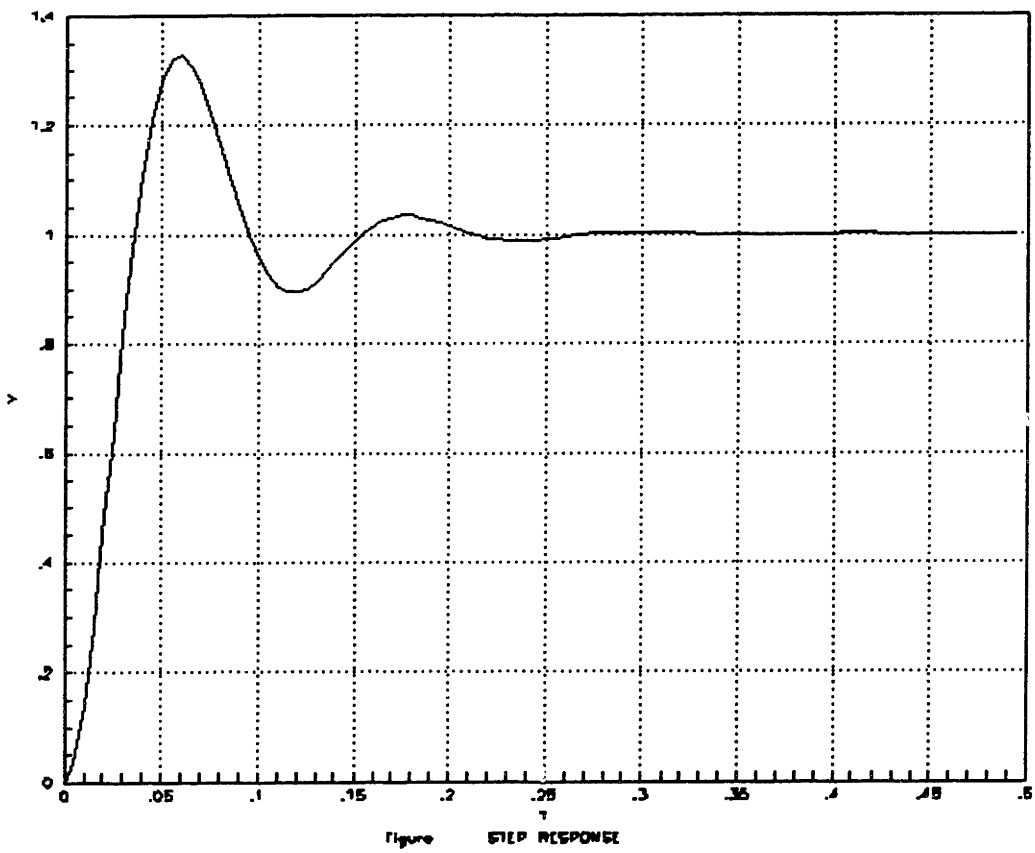

Figure 6-13

Step Response Of The Servo System

input. The unit impulse response of the servo system is shown in Figure 6-14. The response of the system to a set of general inputs is shown in Figure 6-15. The solid line U is the random input signal (White-noise input) and the dotted line Y is the system response. The system response follows very closely the desired command input.

The root-locus of the modelled system is shown in Figure 6-16. As the characteristic equation has two complex roots, the closed loop poles of the system are always in the left half of the s-plane. Hence, no matter how much gain is increased, the system always remain stable. However, if the gain is set at a very high value, the effects of some of the neglected time constants may become important and the system which is supposedly of second order, but actually of higher order, may become unstable.

6.3 STABILITY AND JOINT CLEARANCES

The multiple position problems of series and parallel linked mechanisms were mentioned in Chapters 3 and 5. In the parallel mechanism a given set of joint coordinates results, in general, in several end effector positions. There are singular sets of joint coordinates where the number of positions of the end effector are reduced and the end effector loses a degree of constraint. That is, the motion of the platform in some direction is instantaneously uncontrollable. These sets of joint coordinates must be avoided. Such unstable configurations in the Stewart platform type mechanism are not single points but regions because of the clearance in the joints. Even a very small joint clearance can result in a relatively large region of uncontrollability.

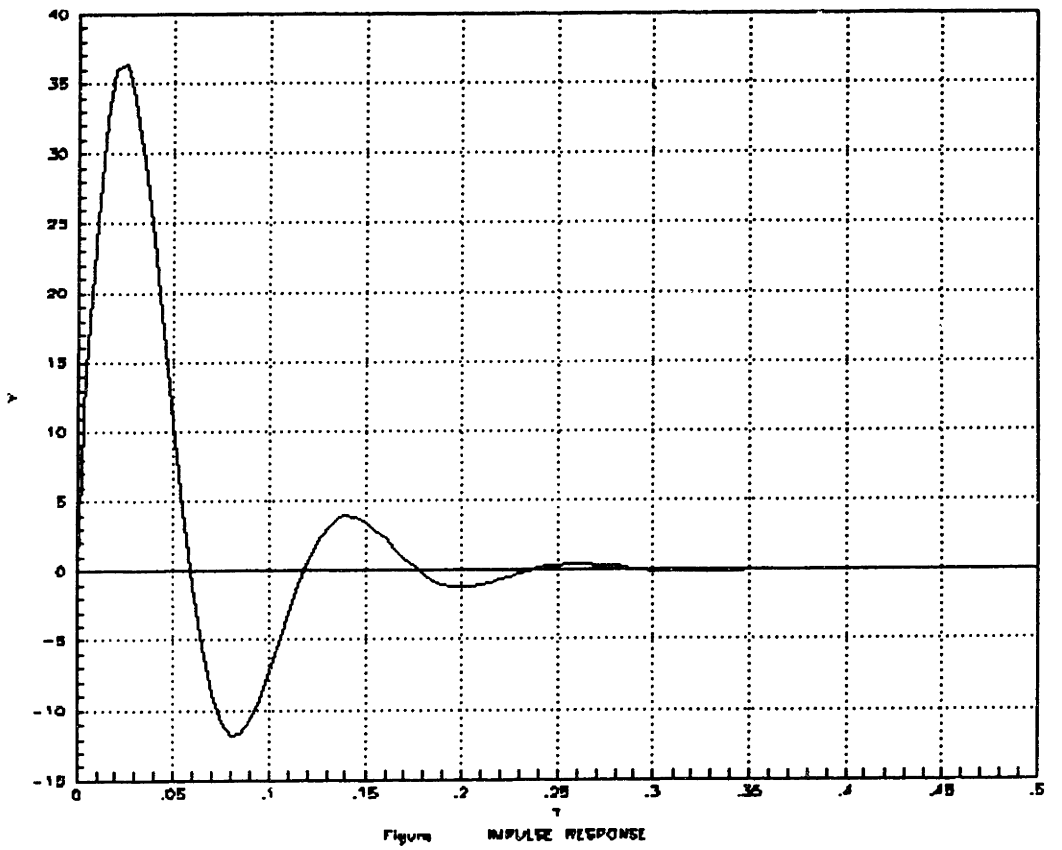

Figure 6-14

Impulse Response Of The Servo System

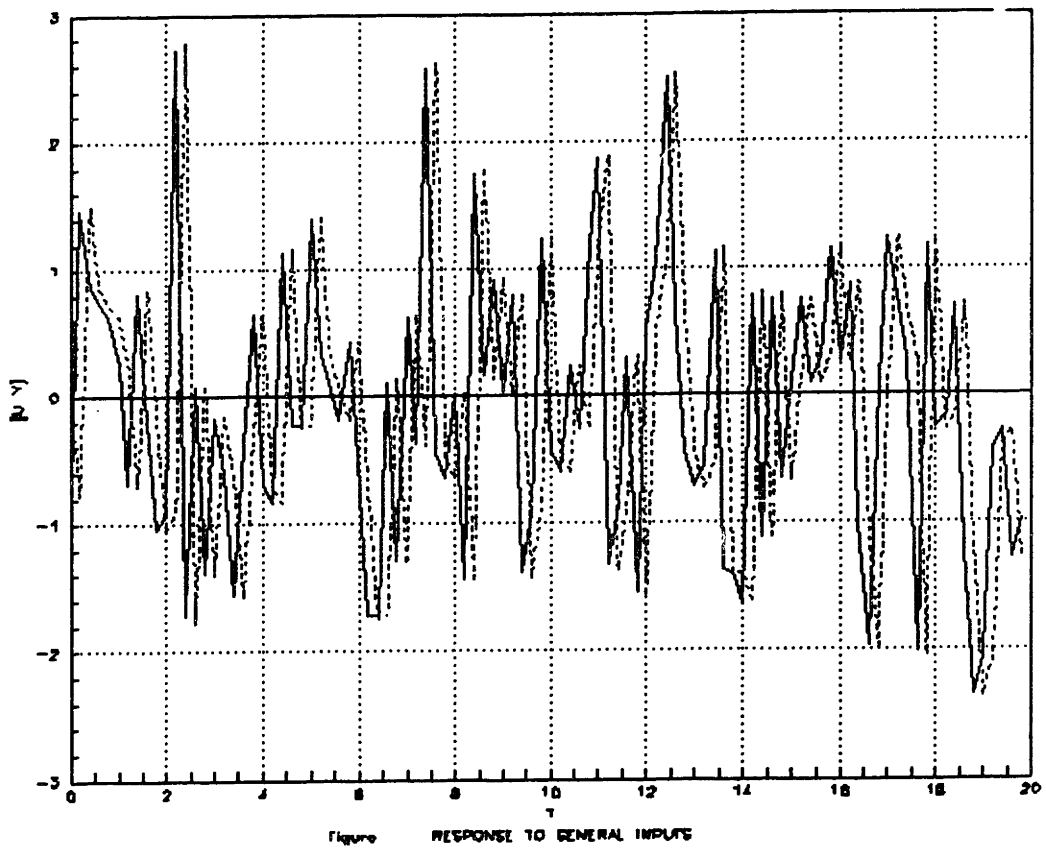

Figure 6-15

Response To General Inputs

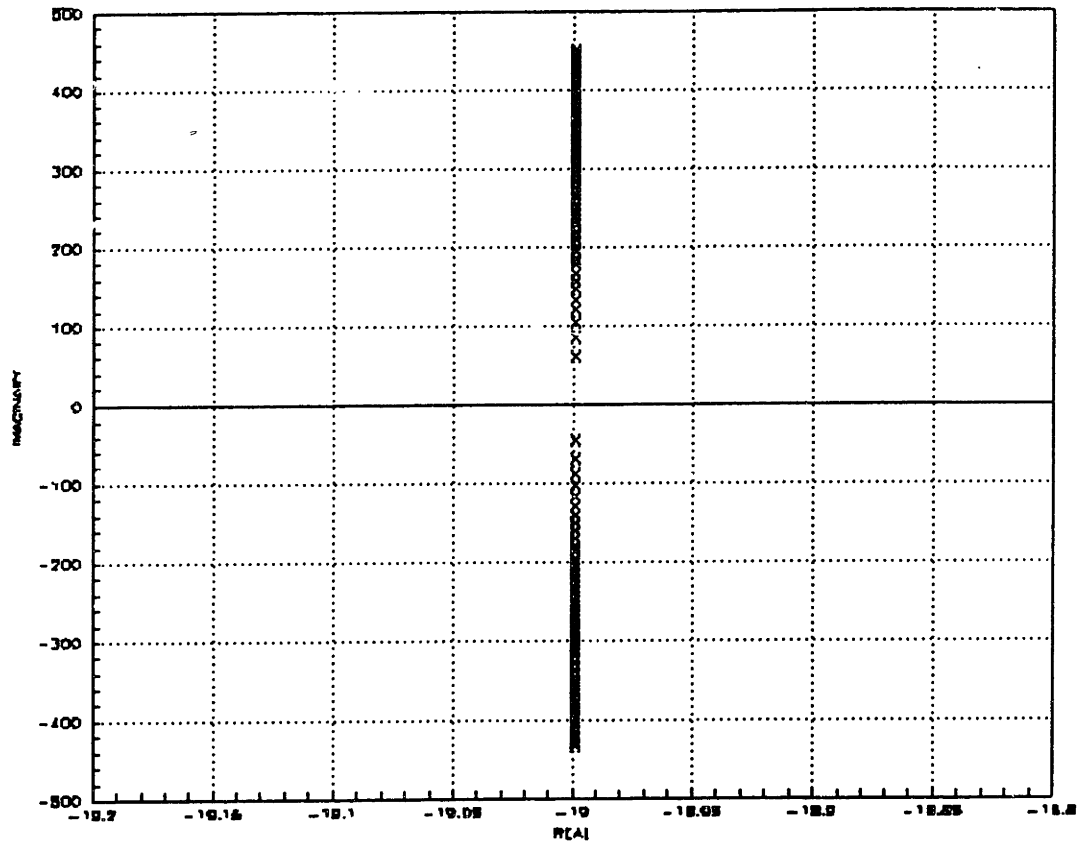

Figure 6-16

Root Locus Of The System

Also, the accuracy with which we can specify the location of the top plate of the platform clearly depends on the clearances in its joints, the rigidity of the platform's structural members, and the dimensional tolerances of its components. The joint clearances and the dimensional errors are associated with the uncertainties in the manufacturing of the various components of the platform.

A practical way to reduce the play in the mechanism is by preloading the platform. The work is continuing to increase the accuracy and the stability of the system [18]. The clearances in all the joints of the platform will be measured and their effects will be incorporated in the control algorithm. Hence, the enhanced control algorithm will be able to counteract the negative effects of the clearances.

CHAPTER 7

SUMMARY AND CONCLUSIONS

7.1 SUMMARY

A six degrees of freedom, parallel linked, platform was designed, built and tested. The hydraulically powered platform's spatial mechanism is used to simulate arbitrary base motions of non stationary-robots.

The platform is controlled by a digital computer and can be operated under either simple position control or admittance control. The platform can be modelled as a mass-spring-damper system and depending on software can be any linear or nonlinear system. The apparent admittance parameters (stiffness, damping, and inertia) of the system can be varied through software such that a wide range of applications can be simulated.

The external forces that are exerted by the robot base on the top plate of the platform are measured by a six degree of freedom force sensor and fed back to the computer. The computer calculates the desired platform position by solving the dynamic equations of motion using numerical integration methods. The position control servo is then given a command by the control software to make the platform follow the computed position profile.

Forward kinematic analysis was also investigated and solved. The solution of the forward kinematics is very important for general position and orientation control of the platform. For a general parallel linkage the forward mapping cannot be specified in closed form and at best is

approximated by a search algorithm implemented on computer. A set of non-linear, mathematical equations were derived using the geometry of the platform and were solved iteratively using multidimensional Newton-Raphson method.

7.2 SUGGESTIONS

The iterative solution of the forward kinematics can be avoided by installing a simple rotary potentiometer on the base U-joint of each actuator. The angular position of each actuator relative to the world coordinates will permit in calculating the forward kinematics in closed form.

Control, stability and the accuracy of the platform can be further improved by modelling the joint clearances and implementing the counteractions to the play in the control algorithm. Continuing work will be dealing with improving the control theory, position accuracy and modelling the non linearities of the physical system.

APPENDIX A

INSTRUMENTATION SPECIFICATION

Page Nos.

APPENDIX A1

HYDRAULIC SUPPLY

The power supply is equipped with a 7.5 horsepower motor (Baldor Electric, model no. GM3311/f971), a constant displacement pump (Paul-Munroe Hydraulics, model no.P328AH21R01), a relief valve (Rexroth, model no. DB15G1-10/5000/5), an accumulator (Greerolator, model no. 20-250TMR-S1/2), two filters (Moog, model nos. HPF-50 and LPF-80-3M), a check valve, a pressure gauge, a 55 gallon oil tank, and 2000 psi. rated tubing and fittings. The unit can deliver a flow rate of 22 gallons per minute at 500 psi pressure.

The hydraulic power supply unit is assembled and delivered by Kennet Corporation. The power supply delivers constant pressure which can be varied by adjusting the relief valve. Mobil Aero HFA (specific gravity = 0.865) is used as hydraulic fluid.

APPENDIX A2

SERVOVALVE SPECIFICATION

Model	= MOOG 62X820
Rated Flow	= 20 gpm $\pm$ 10% (@1000psi)
Rated Signal	= 100 MA (Parallel Coils)
MaxLeakage	= 4cis (@ 1500psi)
Threshold	$\leq$ 1 MA (1%)
Hysteresis	$\leq$ 5 MA (5%)
Null Bias	$\leq$ 1.5 MA (1.5%)
Pressure Centershift	< 3 MA 1000psi-2000psi (3%/1000psi)
Coil Resistance	= 28 Ω

APPENDIX A3

POTENTIOMETER AND FORCE SENSOR

POTENTIOMETER: LONGFELLOW Linear Motion Transducer Type LFS-18/450-OD5

Resistance = 5 KΩ $\pm$ 20%

Linearity = $\pm$ 0.1%

FORCE SENSOR : AMTI Multi Component Transducer Type MC12

Capacity:	F_x, F_y	= 200 lbs
	F_z	= 400 lbs
	M_x, M_y	= 2400 in-lb
	M_z	= 1200 in-lb
Sensitivity:	F_x, F_y	= 6 microvolts/volt-lb
	F_z	= 1.5 microvolts/volt-lb
	M_x, M_y	= 0.6 microvolts/volt-in-lb
	M_z	= 1.3 microvolts/volt-in-lb
Stiffness x (10^{-6}):	60,000 lb/in	
Resonant Frequency:	F_x, F_y	= 300 Hz
	F_z	= 600 Hz

APPENDIX A4

COMPUTER

TYPE : DIGITAL EQUIPMENT CORPORATION PDP 11/73

Processor : 16 bit

Ram : 512 Kb

Operating Systemm : RT11

Language Used : PASCAL

Some timings are given below to help estimate how long a PDP 11/73 and the I/O boards take to do calculations [11].

- 2.5 micro-seconds for 16 bit integer addition and subtraction
- 9 micro-seconds for 16 bit integer multiplication and division
- 25 micro-seconds for single precision real number addition and subtraction
- 28 micro-seconds for single precision real number multiplication and division
- 25 micro-seconds for Analog to Digital (A/D) conversion
- 65 micro-seconds for Digital to Analog (D/A) conversion

APPENDIX B

ENGINEERING DRAWINGS

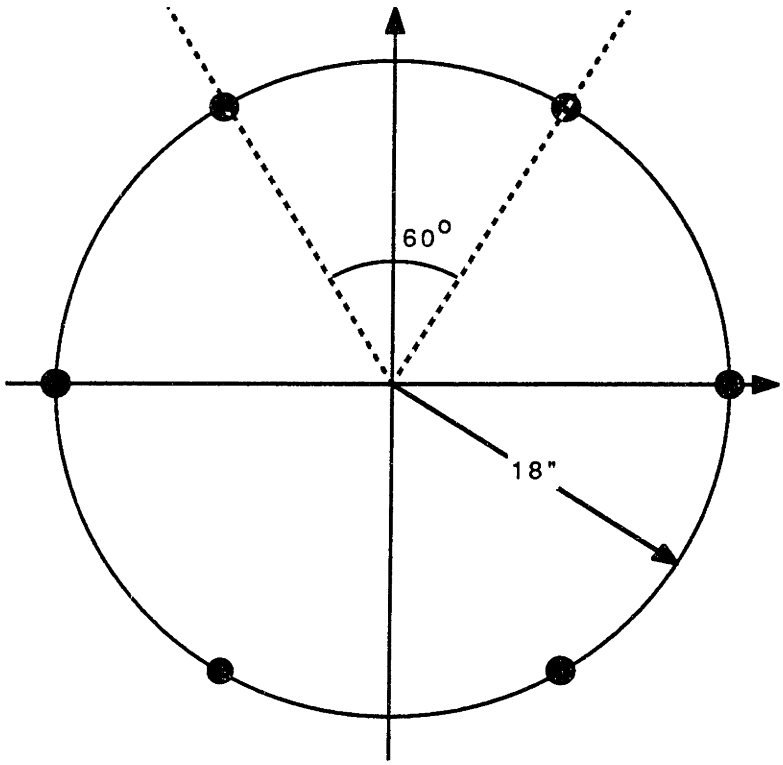

Location of center of base U-joints

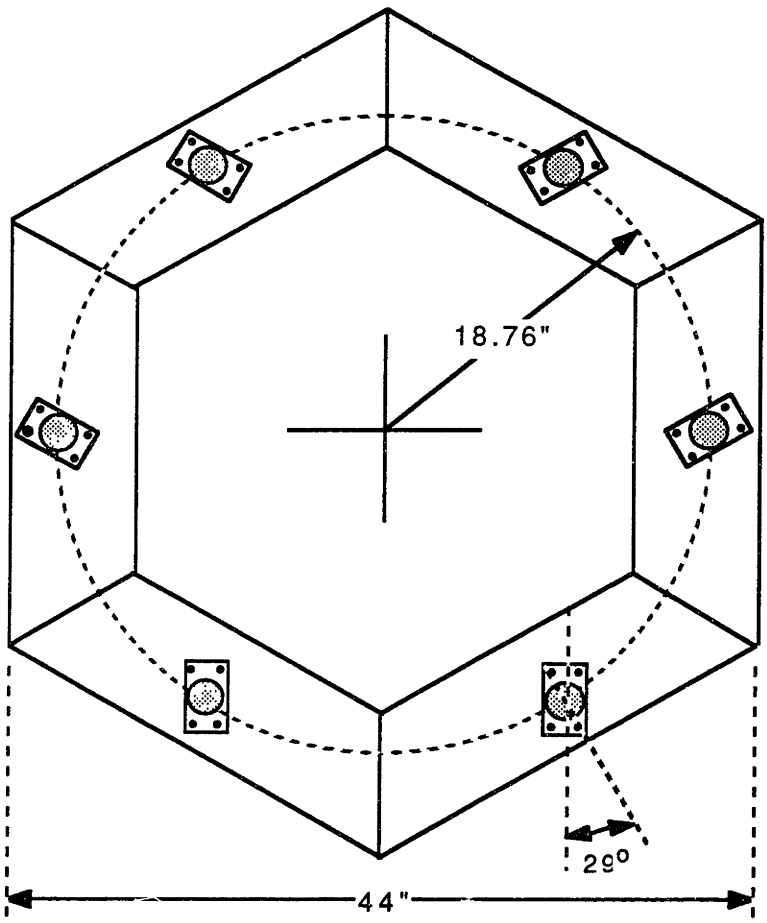

Platform Base

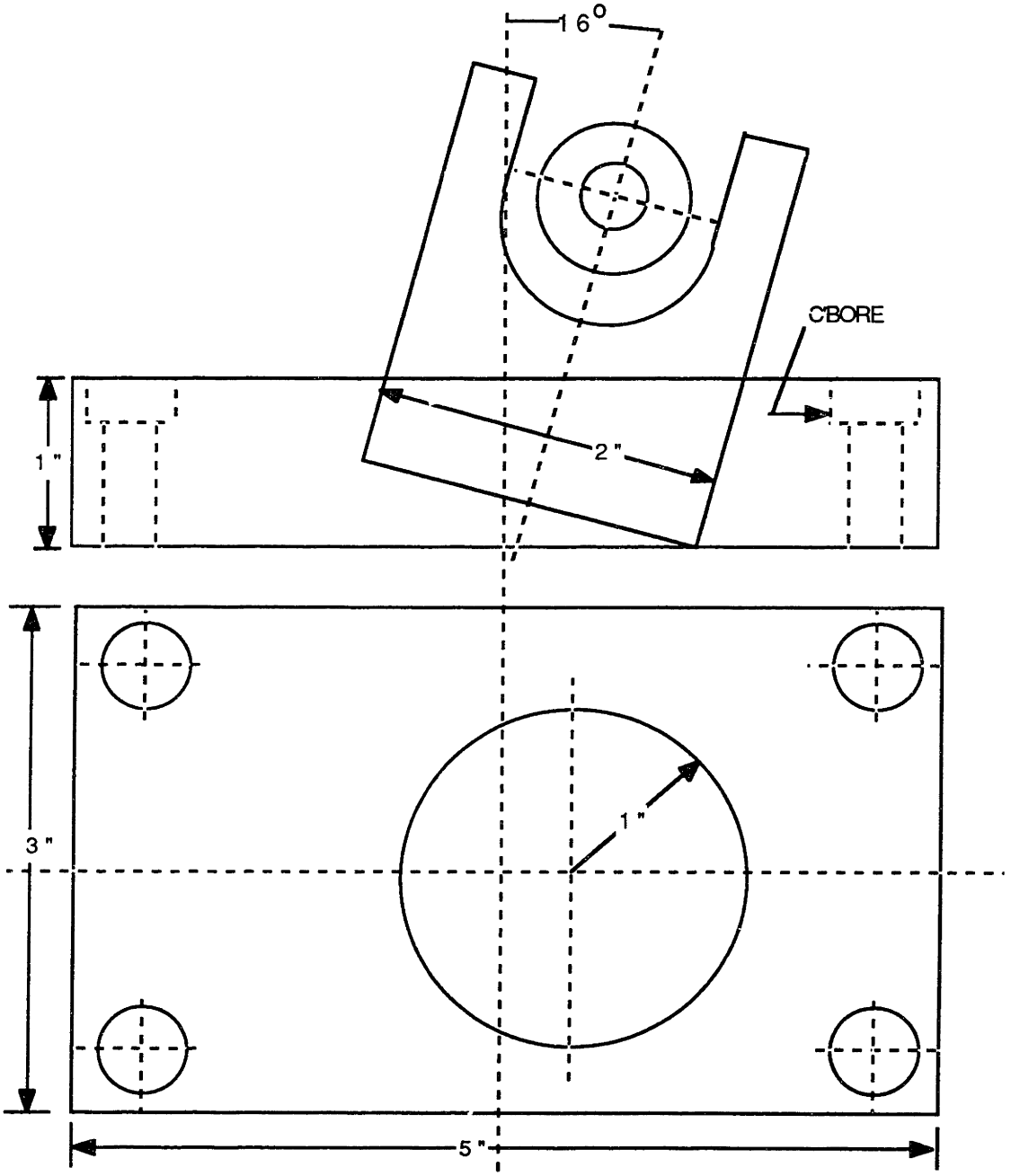

Base Joint and Base Plate

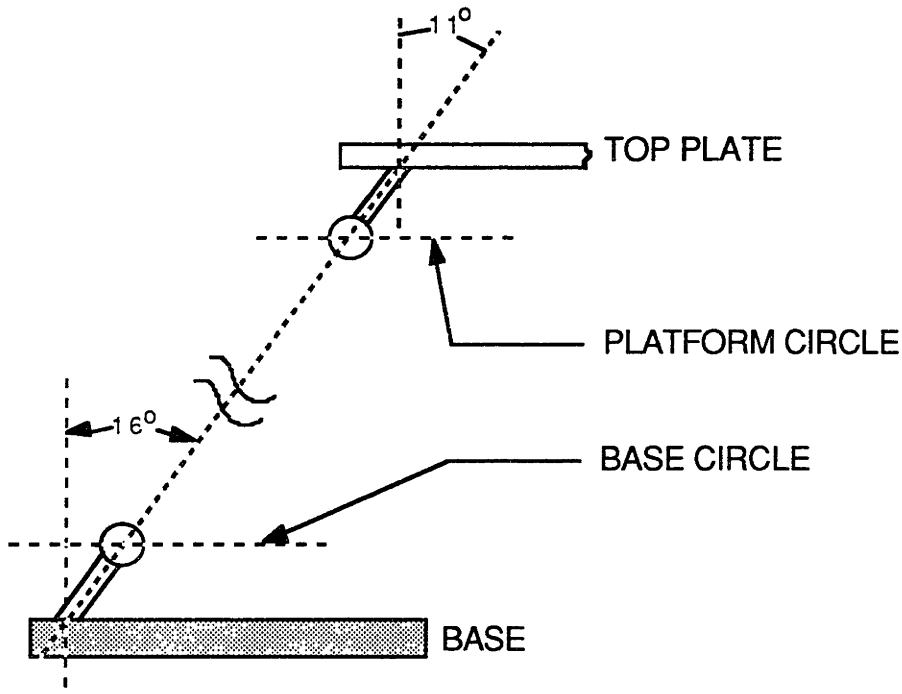

Base and Top Joint Orientation

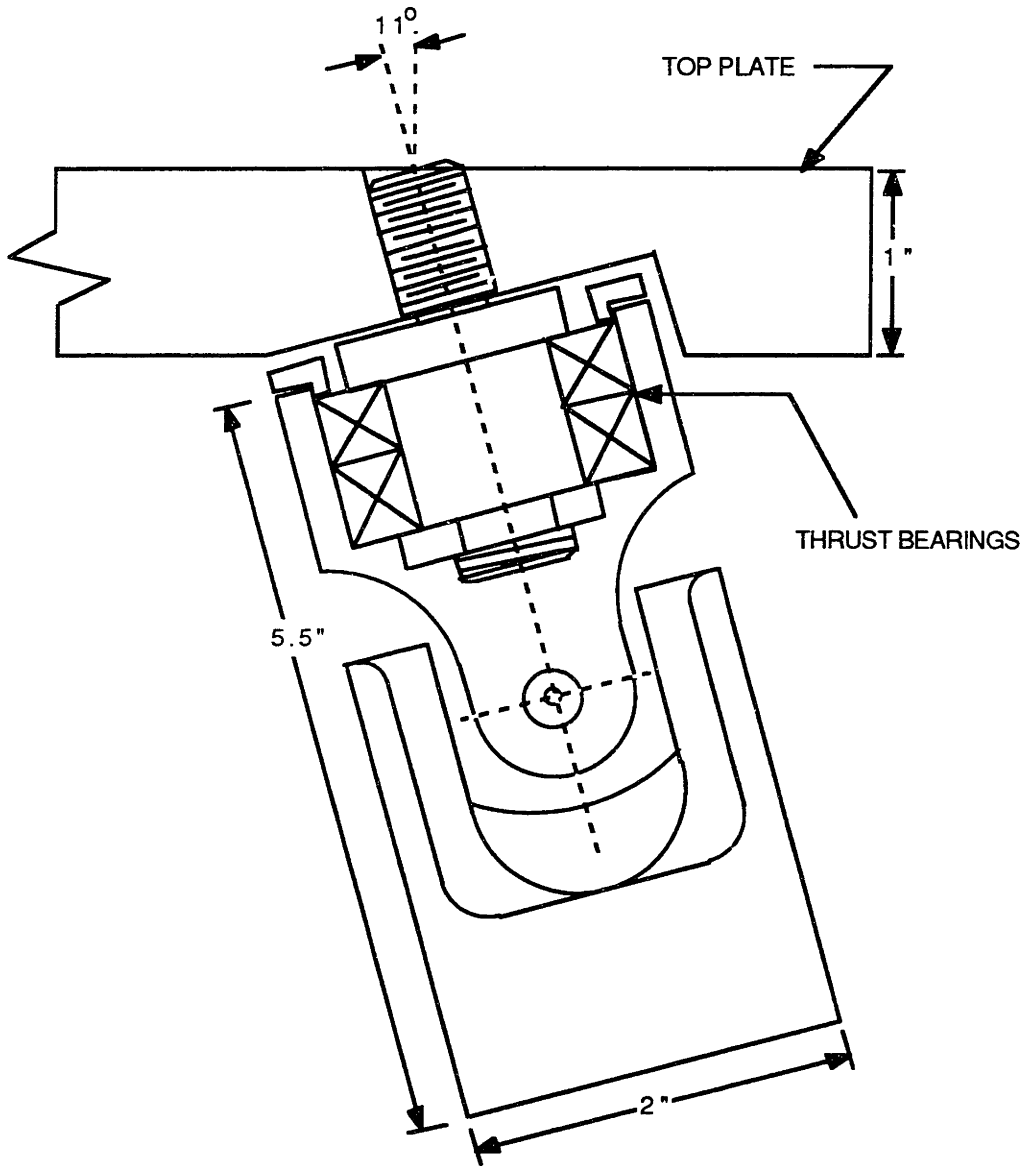

Top Joint Design

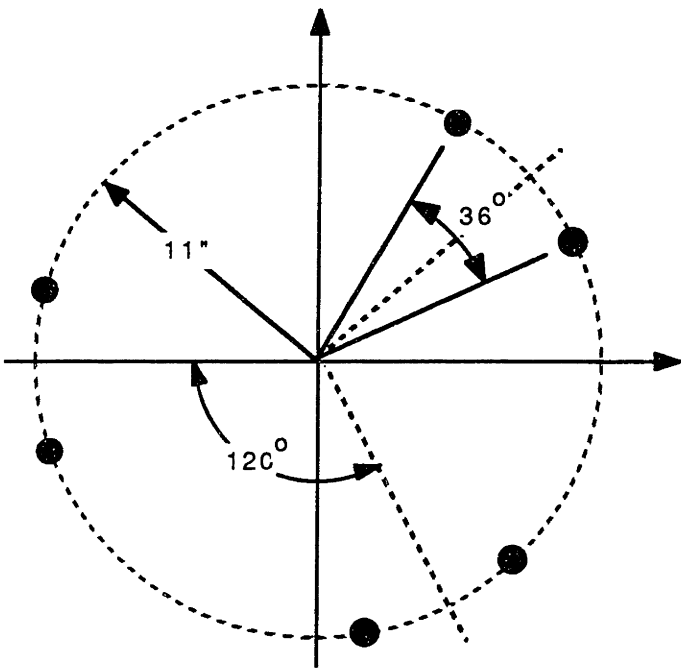

Top Joints Location

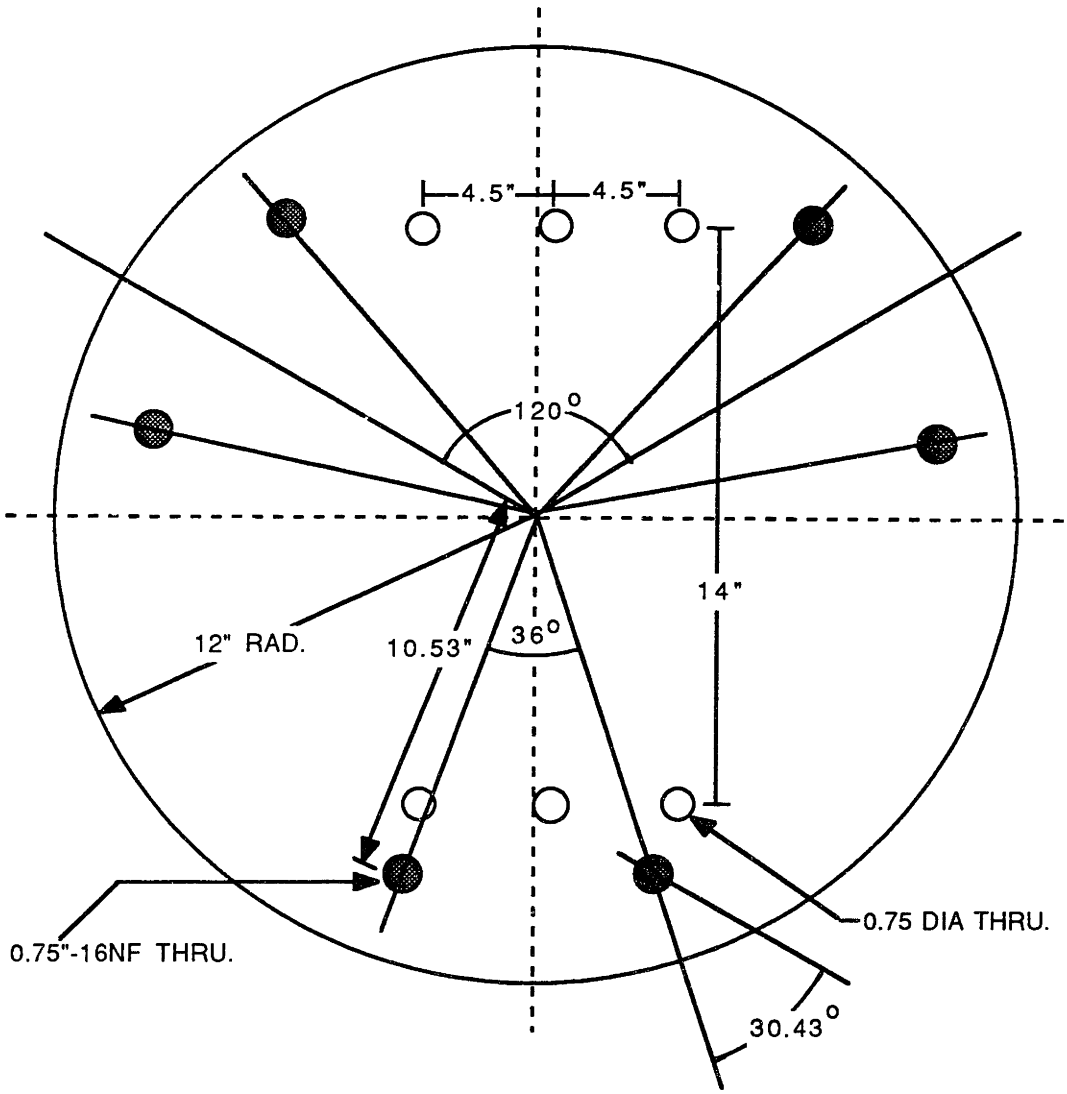

Top Plate Design

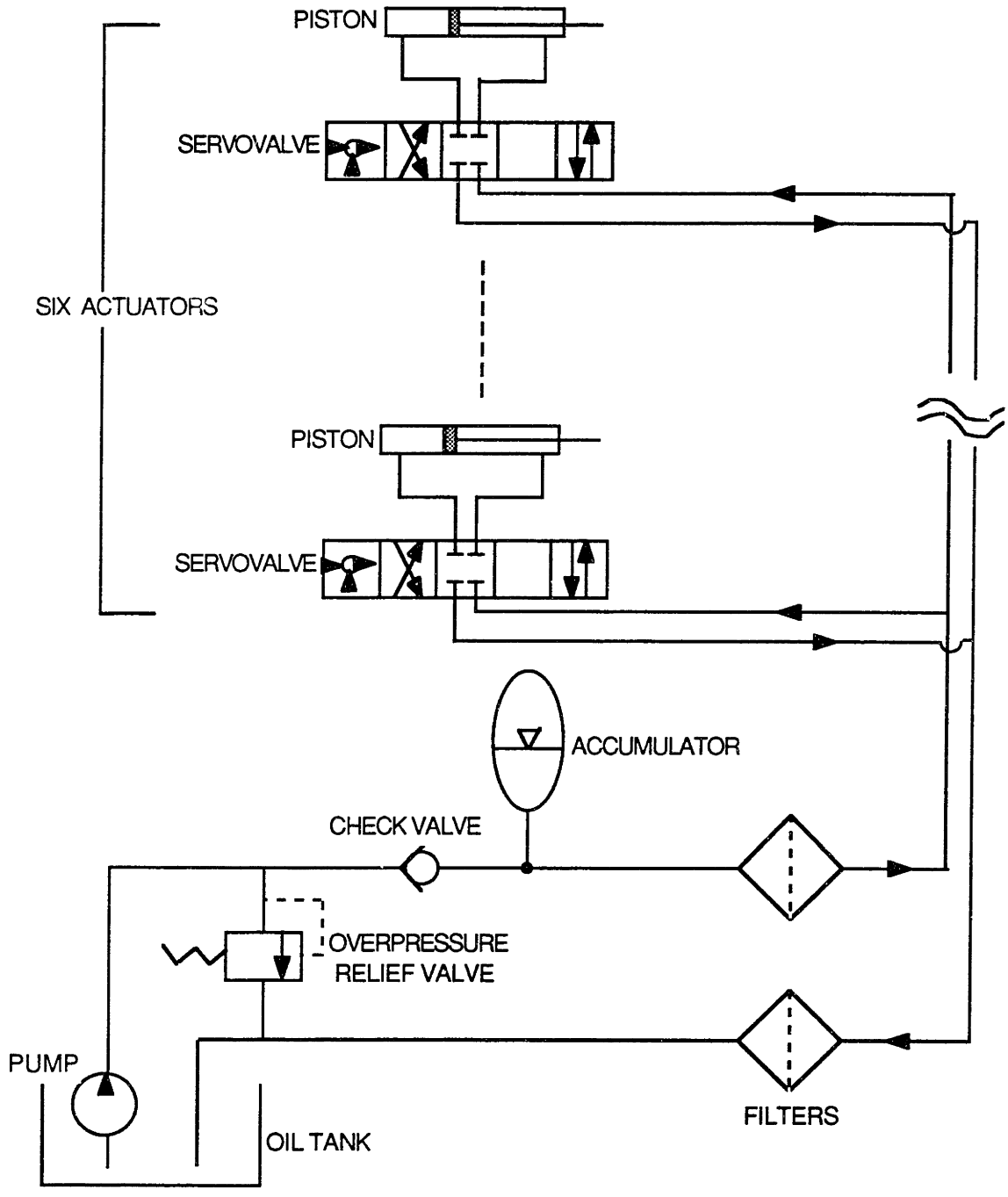

Schematic of Hydraulic Power Supply

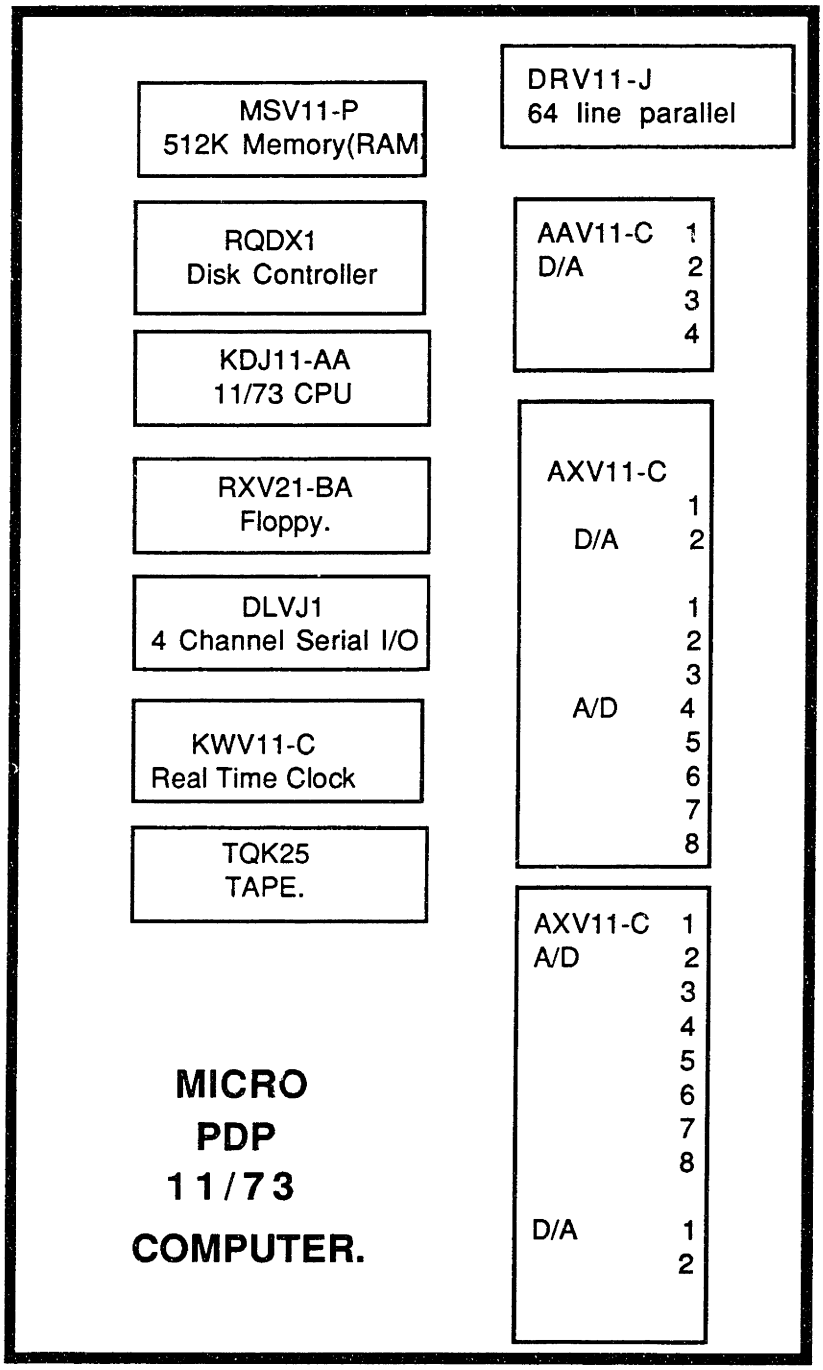

Computer and Relevant Boards

REFERENCES

[1] Tanner, A., "Study of Robotic Manipulators subjected to Base Disturbances", M.S. Thesis, M.I.T., Cambridge, MA., January 1987.

[2] Unimation Inc., "PUMA Robot Series 200 Equipment and Programming Manual", Unimation Inc., Danbury, CT., 1983.

[3] Stewart, D., "A Platform with Six Degrees of Freedom", Proceedings of the Institution of Mechanical Engineers, Vol. 180, Part 1, No. 15, 1965-66.

[4] Fichter, E. F., McDowell, E. D., "Determining the motions of joints on a Parallel Connection Manipulators", Proceedings of the Sixth World Congress on Theory of Machines and Mechanisms, 1983.

[5] Fresko, M., "The Design and Implementation of a Computer Controlled Platform with Variable Admittance", M.S. Thesis, M.I.T., Cambridge, MA., January 1987.

[6] Fichter, E. F., McDowell, E. D., "A Novel Design for a Robot Arm", Advances in Computer Technology, an ASME Publication, 1980.

[7] McCallion, H., Troung, P. D., "The Analysis of a Six Degree of Freedom Workstation for Mechanized Assembly", Proceedings of the Fifth World Congress on Theory of Machines and Mechanisms, an ASME Publication, 1980.

[8] Crandall, S. H., Karnopp, D. C., "Dynamics of Mechanical and Electro-mechanical Systems", Robert E. Krieger Publishing Company, Malabar, Florida, 1985.

[9] McDonald, A. C., "Robot Technology, Theory, Design and Applications", Prentice Hall, Inc., Englewood Cliffs, NJ, 1986.

[10] Shigley, J. E., Mitchell, L. D., "Mechanical Engineering Design", McGraw Hill Book Company, New York, 1983.

[11] Digital Equipment Corporation, "LSI-11 Analog System User's Guide", Bulletin No. EK-AXV11-VG-003, Digital Equipment Corporation Educational Services, Bedford, MA, 01730, 1982.

[12] Paul, R. P., "Robot Manipulators: Mathematics, Programming and Control", The MIT Press, Cambrige,.1982.

[13] Asada, H., Slotine, J. J., "Robot Analysis and Control", John Wiley and Sons, NY, 1986.

[14] Yang, D. C. H., Lee, T. W., "Feasibility Study of a Platform type of Robotic Manipulator from a Kinematic Viewpoint", Journal of Mechanisms, Transmission, and Automation in Design, Vol. 106, June 1984.

[15] Alizade, R. I., Tagiyev, N. R., "Kinematic Analysis of High Class Multi-loop Spatial Mechanisms, Robots and Manipulators", Proceedings of the &th World Congress on Theory of Machines and Mechanisms, 1987.

[16] Thayer, W. J., "Transfer Function For Moog Servovalves", Bulletin No. 103, Moog Inc. Controls Division, East Aurora, NY 14052, 1965.

[17] Ogata, K., "Modern Control Engineering", Prentice Hall, Inc., Englewood Cliffs, NJ, 1970.

[18] Stelman, N. M., "Design and Control of a Six-Degree-of-Freedom Platform with Variable Admittance", M.S. Thesis, M.I.T., Cambridge, MA, May 1988.